# Stewart Platform: Design and Construction

Henrik Hov
Håvard Mesøy Mannes
Markus Thorsnes

Bachelor's thesis in Mechanical Engineering
Bergen, Norway 2022

Høgskulen på Vestlandet


# Stewart Platform: Design and Construction

Henrik Hov
Håvard Mesøy Mannes
Markus Thorsnes

Department of Mechanical- and Marine Engineering
Western Norway University of Applied Sciences
NO-5063 Bergen, Norge

IMM 2022-M06

Høgskulen på Vestlandet
Institutt for Maskin- og Marinfag
Inndalsveien 28,
NO-5063 Bergen, Norge



| | |
|---|---|
| Norsk tittel: | Stewart Plattform: Design og Konstruksjon |
| Author(s), student number: | Henrik Hov, 585081<br>Håvard Mesøy Mannes, 585072<br>Markus Thorsnes, 161824 |
| Study program: | Mechanical Engineering |
| Date: | May 2022 |
| Report number: | IMM 2022-M 06 |
| Supervisor at HVL: | Thorstein R. Rykkje |
| Assigned by: | Western Norway University of Applied Sciences and Palfinger Marine |
| Contact person: | Thorstein R. Rykkje |
| Antall filer levert digitalt: | 1 |

# Preface

This work has been carried out in the framework of a bachelor thesis at Western Norway University of Applied Sciences (WNUAS) and the Department of Mechanical- and Marine Engineering, in the field of a Mechanical Engineering program in Bergen, Norway. The bachelor thesis is a part of a doctoral project for Thorstein R. Rykkje at WNUAS and in cooperation with Palfinger Marine. A big thanks to the Frank Mohn Foundation for providing funding to this project. Without their help, the thesis would not be possible.

We would like to take the opportunity to give special thanks to our supervisor and doctoral student Thorstein R. Rykkje, who provided guidance and expertise throughout the project. We would like to thank Research Technician Kjetil Gravelsæter, Staff Engineer Frode W. Jansen and Chief Engineer Harald Moen for helping us through the construction and being a part of decision-making throughout the Stewart platform project.

- Henrik Hov, Håvard Mesøy Mannes and Markus Thorsnes


# Abstract

In this thesis, a Stewart platform has been designed, produced, and constructed. This Stewart platform is required to have six degrees of freedom, the same amount that appears on a ship at sea. This allows for the creation of artificial waves, only using motions made by the Stewart platform. Placing a test object on top of the Stewart platform and then run various simulations, enables the experience of wave motion on the object before it is mounted on a ship. These simulations can tell if the object needs further development or not. The goal is to design a fully functional Stewart platform that creates wave motion with a high level of accuracy, which will be used for testing and research on various objects.

As a part of this thesis, an adjustable fastening method has been developed. The Stewart platform is intended to have a crane attached as a part of Thorstein R. Rykkje's doctoral project. The platform must be able to have other objects attached as well, with various geometries. A design like this makes the Stewart platform accessible for a diversity of objects.

The Stewart platform has been designed using Creo Parametric, analysed using ANSYS, and then constructed and assembled using fasteners. A selection of designs has been drafted and different choices are explained throughout the report. The Stewart platform is assembled with multiple parts, each of which has been discussed and optimized for its purpose. Dimensions have been calculated using the maximum load while the Stewart platform operates at a maximum angle. A factor of safety from the requirement list has also been taken into account.

# Sammendrag

I denne oppgaven er det designet, produsert og konstruert en Stewart plattform. Stewart plattformen er pålagt å ha seks frihetsgrader, som er det samme antallet som forekommer på skip til sjøs. Dette tillater å simulere kunstige bølger, bare ved å bruke bevegelsene laget av Stewart plattformen. Et testobjekt plassert på toppen av Stewart plattformen, som det deretter blir kjørt simuleringer på, tillater opplevelsen av bølgebevegelser før den eventuelt blir montert på et skip. Disse simuleringene kan fortelle om objektet trenger videreutvikling eller ikke. Målet er å lage en funksjonell Stewart plattform som simulerer bølgebevegelser med høy nøyaktighet, som vil bli brukt til testing og forskning på ulike testobjekter.

Som en del av denne oppgaven er det utviklet en justerbar festemetode. Stewart plattformen er tiltenkt å ha en kran montert som en del av Thorstein R. Rykkje's doktorgradsprosjekt, men Stewart plattformen må også kunne ha andre gjenstander festet, med ulike baser. Et design som dette gjør Stewart plattformen tilgjengelig for et mangfold av objekter.

Stewart plattformen er designet i Creo Parametric, analysert i ANSYS og deretter konstruert og satt sammen ved hjelp av bolter og muttere. Et utvalg av design er utviklet og ulike valg er forklart gjennom denne oppgaven. Stewart plattformen er satt sammen av flere deler, som hver og en har blitt drøftet og optimalisert. Dimensjoner er beregnet ved hjelp av maksimal belastning mens Stewart plattformen opererer i maksimal vinkel. En sikkerhetsfaktor fra listen av krav er også tatt i betraktning.

# Contents

# 1 Introduction

## 1.1 Background

The Stewart platform is a parallel redundant manipulator that involves a configuration of six degrees of freedom (DOF). Each degree of freedom corresponds to an actuator [1]. A special mechatronic system utilized for motion control and precise positioning was designed by D. Stewart. The Stewart platform was originally used as a flight simulator in 1965 [2]. Today's use in the industry ranges beyond solely flight simulators. Machine tool technology, satellite dish positioning, wave simulation and wave compensations are some of the many current applications for a Stewart platform. A top platform and bottom base are linked together using joints, shafts, and linear actuators. Different variants of actuators vary from electric, pneumatic, and hydraulic.

A solid Stewart platform is necessary to withstand various loads and forces which occur when simulating different motions. The Stewart platform can be modified for specific applications.

## 1.2 Problem description

This thesis reviews the process of designing and constructing a Stewart platform, seen in Figure 1. The project is classified as a development project since the main goal is to design and construct a Stewart platform. The specific Stewart platform designed in this thesis must be tailored toward simulating wave motion.

The Stewart platform must be able to attach objects with different geometry on top of the construction. An ideal test object would be a crane. If a crane could be attached, research on offshore crane motion without using the wave tank at WNUAS would be possible.

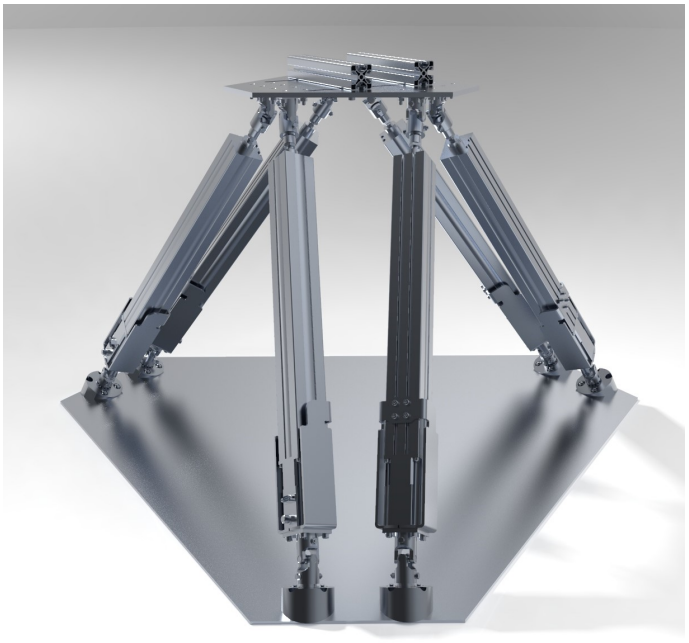

Figure 1: Stewart platform.

To reach the main goal, a primary objective is set, focusing on designing a cost-efficient Stewart platform. Reaching the set objective, several engineering software are utilized. The software used throughout the project is mainly PTC Creo [3] and ANSYS [4], which is used to design- and optimize models with stress- and deformation analyses. Calculations are mostly performed using MATLAB [5]. In accordance with cost-efficiency, an effort is made to use as much material from WNUAS as possible to prevent unnecessary spending from the available budget.

For this project, a list of requirements is given below:

- Six DOF
- Max load: 60 kg
- Fits on an Euro-pallet
- Adjustable fastening method
- Safety factor of two for the load
- Simulate motion that compares with data from the MarinLab at WNUAS

## 1.3 Approach

The thesis is carried out, with some deviations, using the current approach:

1. Thorough research in various aspects to decide the design
2. Researching a hydraulic system, as this is desired
3. Calculate early design thoughts and drafts
4. Use 3D modelling to draw and assemble the construction
5. Conduct stress analyses on exposed components and structure
6. Order actuators, bearings, universal joints and other necessary components
7. Bring drawings to engineers at the workshop to produce desired components
8. Assemble and construct the Stewart platform

The participants usually met at the university, which enabled healthy discussions and continual teamwork throughout the Bachelor project. Being able to arrange face to face meetings with the engineers at the workshop and supervisor was a privilege, something that was not taken for granted during the pandemic.

# 2 Method

*"The purpose of research is to produce valid and credible knowledge about reality. To explain this the researcher must have a strategy of moving forward. This strategy is method"* [6]. A solid strategy is a necessity to produce a dependable product. The Stewart platform is a development project; thus, the strategy embodies a practical- and theoretical approach. Since the Stewart platform will be produced at the workshop at the university, most of the project will consist of a practical approach. However, the practical approach is based on a solid theoretical foundation.

## 2.1 Theoretical approach

Rotational- and translative motion is vital for understanding wave dynamics. Wave dynamics are analysed and mentioned throughout the thesis. In Figure 2 below, is a coordinate system of an X-, Y-, and Z-axis with a frame locked in the centre of mass. Translative motion is any motion of the frame along the X-, Y-, or Z-axis, or any combination of the three axes. These are usually described as surge, sway, and heave. Rotational motion is any motion that rotates about the X-, Y-, or Z-axis, or any combination of the three axes. The rotational motions are called yaw, pitch, and roll. A translative motion along one of the axes corresponds to one DOF. Using the same coordinate system with rotational- and translative motion along all axes, motion can be visualized for a body with six DOF.

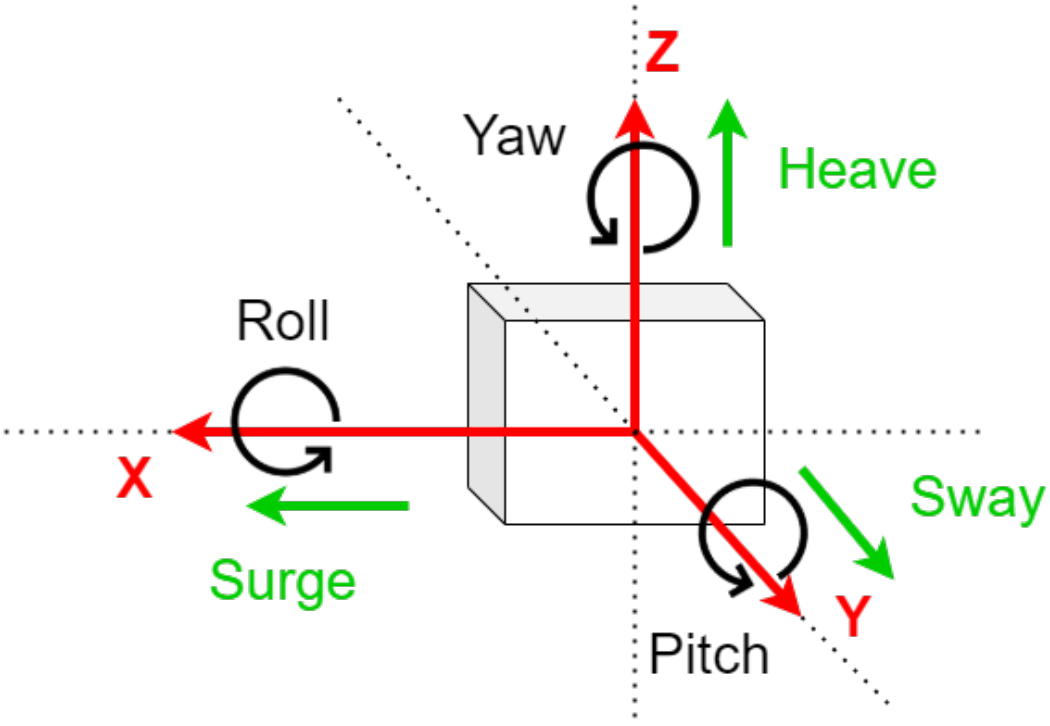


Figure 2: Overview of rotational- and translational motion, inspired by [7].

### 2.1.1 Kinematic analysis

Six degrees of freedom are the foundation of a Stewart platform. Calculating six DOF uses equations and information from an article published by D. Stewart [2].

Each leg between base and platform has been divided into two separate members, shown in the kinematic diagram in Figure 3. One member corresponds to one line between each circle in the vertical direction. The platform and base also count as each member. Adding all lines between the circles, including base and platform, the total number of members is 14. The number of degrees of freedom in the joints is equal to 36. One joint corresponds to one circle. The total number of joints is 18.

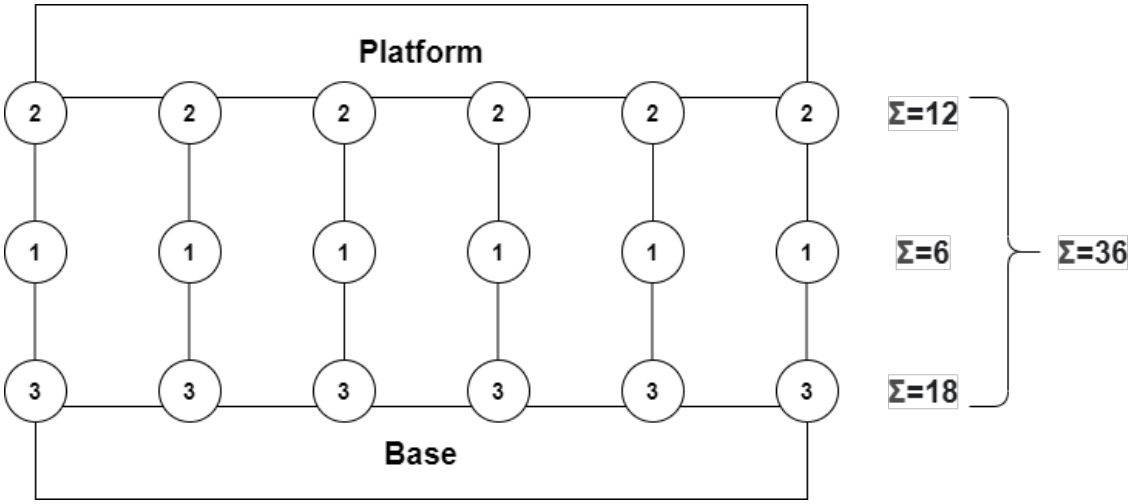


Figure 3: Kinematic diagram of mechanism, inspired by [2].

Thus

$$F = 6\,(n-1) - \sum_{1}^{g} (6-f)\,. \tag{1}$$

Where F = resulting degrees of freedom in system
f = number of degrees of freedom of joints
n = number of members
g = number of joints

As the system can be locked by turning off the actuators, a simplified version of the expression can be written:

$$F = 6\,(n-1) - 6g + f \tag{2}$$

Inserting the corresponding values from Figure 3 into equation (2)

$$F = 6\,(14-1) - 6 \times 18 + 36 = 6 \tag{3}$$

Equation (3) confirms that the system consists of six degrees of freedom.

### 2.1.2 Wave dynamics

Simulating wave motion using the Stewart platform requires certain values from parameters such as range, speed, and acceleration. The MarinLab supplied a total of three models with multiple data sets [8] containing values for each parameter mentioned above. Measurements visualized using MATLAB are made to give an approximation of the respective parameters. The thoroughly selected data sets contain some of the largest wave simulations performed in the wave tank to give the highest possible value of the parameters. If the linear actuator parameters are calculated to perform close to the parameters supplied by the MarinLab, it is reasonable to assume that the motion can be replicated using the Stewart platform.

The three supplied models are “Goliath” and “Tideland buoy” in a 1/4 scale and 1/8 scale. The data gives values such as time, X-, Y- and Z positions, yaw-, pitch-, and roll angles. From the data, 3D position vectors are formed and differentiated into velocity- and acceleration unit vectors. The magnitudes of these vectors represent the speed and acceleration as scalars. To calculate the total velocity combining the translational- and rotational motion, equation (4) is utilized.

$$V = r\omega \times \frac{2\pi}{360} \tag{4}$$

Where V = velocity [mm/s]
r = radius of platform [mm]
$\omega$ = angular velocity [radians/s]

The constant converts radians to degrees. In Figure 4, the velocity from equation (4) is solved and displayed. This data is used as a spectre to visualize how the floating object moves during a time interval. Some of the maximum- and minimum velocity were assumed negligible due to error of measurement.

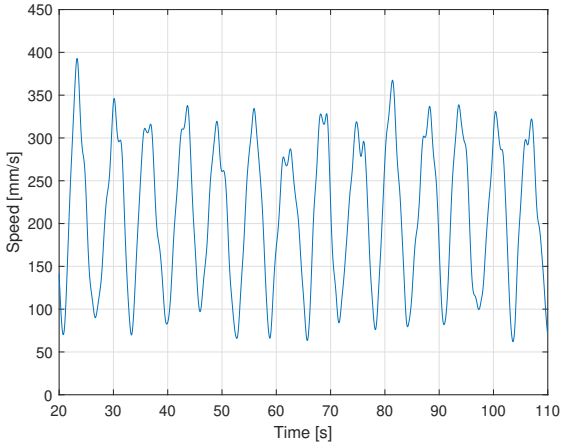


(a) Tideland Buoy 1/8.

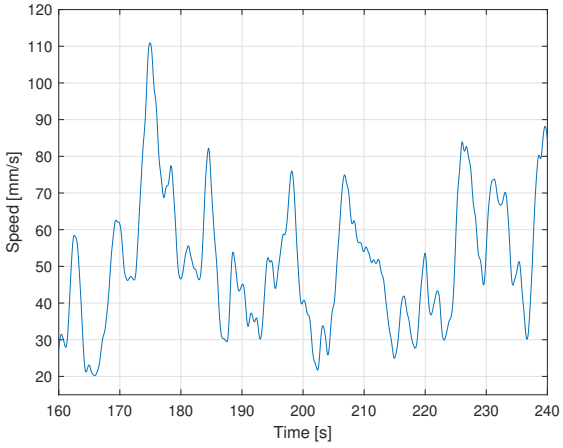


(b) Goliath.

Figure 4: Combined translational- and rotational motion for two data sets.

The interval of the Goliath analysis is longer than a thousand seconds, and therefore, an excerpt from an arbitrary period is shown. In Figure 4a, high values of the Tideland Buoy 1/8 are presented. The Stewart platform will not be able to simulate these waves. Having a peak speed of 110 mm/s for the Goliath, and a mean value of around 250 mm/s for the Tideland Buoy 1/8, a middle value has to be determined. The middle value is used for further dimensioning in Section 2.2.3.

The reason for the drastic value difference between the two analyses is most likely due to the geometry of the objects. The barge from Goliath is long in terms of length while the Tideland Buoy is spherical shaped. As a result, from different geometries, the object's motion along the waves results in different patterns.

In Figure 5 below, heave movement has been analysed. The object moves from -200 mm up to roughly 50 mm as seen in Figure 5a. Heave movement analysis seen in Figure 5b has a maximum of about 10 mm and a minimum of -110 mm. The total travel distance strictly in Z-direction from minimum to maximum is about 250 mm for Tideland Buoy 1/4 and 120mm for Tideland Buoy 1/8.

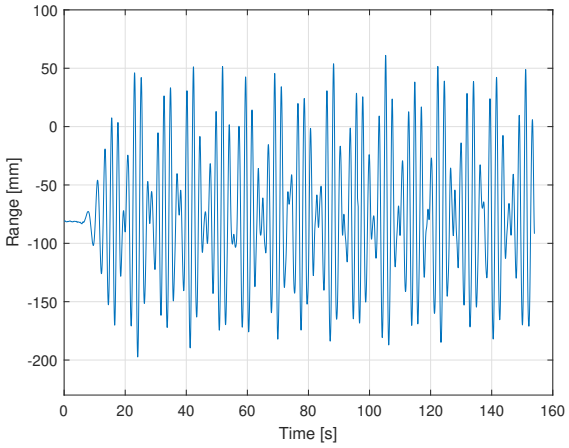


(a) Heave analysis of Tideland Buoy 1/4.

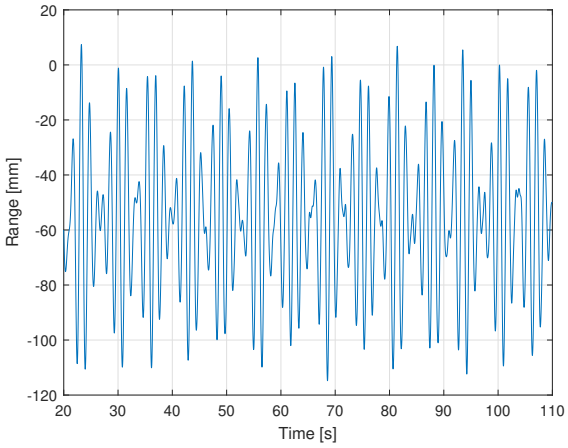


(b) Heave analysis of Tideland Buoy 1/8.

Figure 5: Heave comparison of Tideland Buoy.

Knowing the total travel distance is a key factor as it determines the stroke length of the linear actuators. The heave analysis moves strictly in Z-direction while the actuators are placed on the base at an angle. The actuators operate between 55° - 65° while lifting and lowering in heave direction. The angles must be considered when selecting stroke length. Imagine the simplified triangle in Figure 6 is resembling a cut of the Stewart platform, where:

x = stroke length of actuators

$\theta$ = operating angle for the actuators

h = heave analysis/height between platform and base

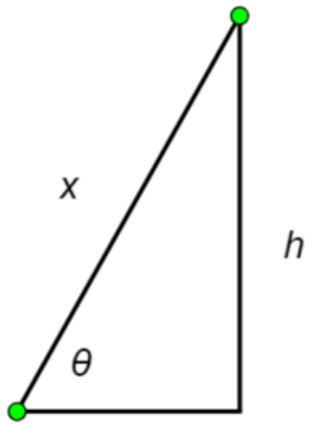


Figure 6: Stroke length dimensioning.

$$x = \frac{h}{\sin\theta} \tag{5}$$

Inserting the maximum angle of 65°, using trigonometry from Figure 6 and maximum heave data into equation (5)

$$x = \frac{250mm}{\sin 65} = 276mm \tag{6}$$

Based on the value from equation (6), the actuators have to be longer than the analysed heave, as the actuators are placed at an angle.

### 2.1.3 Visualization using MATLAB

The Stewart platform has motions that are produced by a combination of movements from multiple actuators, which implies that the platform's positions will vary. Visualizing the different positions gives a better understanding of possibilities and limitations when operating with six DOF. Using MATLAB as an experiment tool, combined angles and positions can be visually represented. Adjustments are made from the original script, to present a Stewart platform that resembles the dimensions for this project [9]. Figure 2 is a indicator of how a ship behaves at sea, while Figure 7 displays these same movements on a Stewart platform.

The default position is displayed in Figure 7a, where Z = 1, X = 0, Y = 0, and Yaw = 90°, Roll = 0°, Pitch = 0°. In Figure 7b strict movement along the Y-axis is visualized. This is also called sway. Based on all analysed data sets acquired from MarinLab, roll and pitch on the test-object did not exceed $\pm$ 10°, while this Stewart platform is allowing for $\pm$ 25°. Figure 7c displays roll. Furthermore, analysed data for yaw did not exceed $\pm$ 20° while the Stewart platform allows for a $\pm$ 40° rotation from the default position, as seen in Figure 7d.

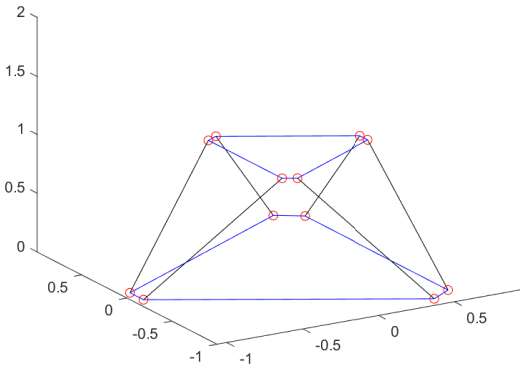

(a) Z = 1 (normal position).

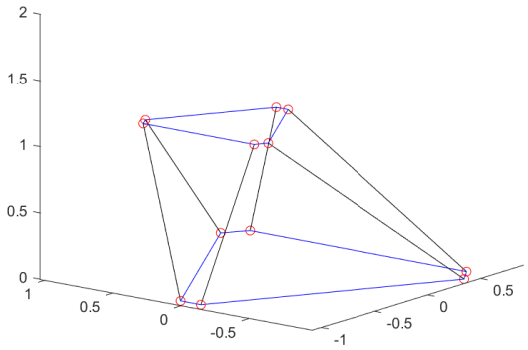

(b) Y = 0.5.

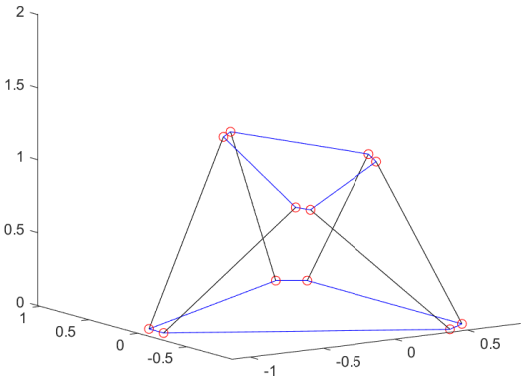

(c) Roll = 25°.

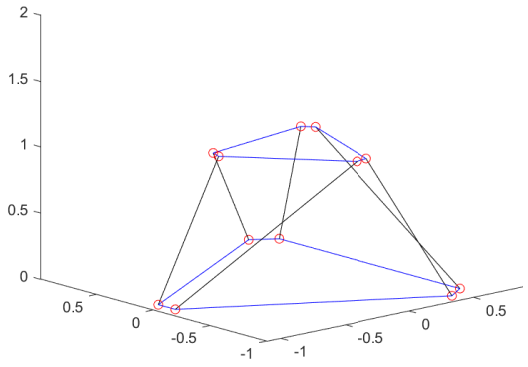

(d) Yaw = 130°.

Figure 7: Display of the kinematics in a Stewart platform for various positions.

## 2.2 Practical approach

The practical approach was mainly centralized around the engineering software used throughout the study course and the work executed in the workshop. The theoretical approach was used as a foundation while further calculations were carried out by combining the use of Creo Parametric and ANSYS. In the following section, various exercises and approaches are described.

### 2.2.1 Budget

The greatest expense of the project was the linear actuators, including all their corresponding components. Both hydraulic and electrical solutions were available, and considering the project was given a budget of 200 000 NOK by the Frank Mohn foundation, both solutions were within price range. Hydraulic systems are superior in strength and speed. However, they are more complicated, less efficient, less environmentally friendly, and more expensive. Table 1 shows how the price varies between an electric- and hydraulic-driven system. In addition, RS Components offered an academic discount for the electric actuators. The discount caused the electric actuators to be cheaper, which elevated the project toward the objective regarding cost efficiency.

**Hydraulic**

| Component | Quantity | Price [NOK] |
|---|---|---|
| Actuator w/motor | 6 | 5 200 |
| Pump | 1 | 35 000 |
| Electric motor | 1 | 12 000 |
| Proportional-valve | 1 | 72 743 |
| Tank | 1 | 6 250 |
| Valve cable | 2 | 2 112 |
| Hose (12m w/fittings) | 6 | 334 |
| Return-filter | 6 | 1 300 |
| Oil-cooler (230V) | 1 | 8 750 |
| Various parts (manometer etc.) | 1 | 11 000 |
| **Sum** | | **190 973** |

**Electric**

| Component | Quantity | Price [NOK] |
|---|---|---|
| Actuator w/motor | 6 | 7 757 |
| Controller | 1 | 5 000 |
| Encoder cable | 6 | 498 |
| Motor cable | 6 | 566 |
| Adapter kit | 6 | 467 |
| **Sum** | | **60 728** |

Table 1: Price comparison table between hydraulic- and electric driven system.

### 2.2.2 Design

Every design was made using PTC Creo, while MATLAB and ANSYS were applied for determining different dimensions. Comparing the work from similar products and drawing new design drafts was a time-consuming phase of the project. Preparing various design solutions while collecting benefits from each of them. Collectively, this results in a valid final design draft. The design was put together in the virtual model by assembling parts from the base to the platform in an assembly file.

The Stewart platform has been designed with a component that contains a weak spot. This is ultimately to ensure that if any component fails, it is a cheap component that is easy to replace. The part is designed and produced with a notch and is expected to fail before the expensive parts. In addition, the part is available to manufacture at the university. Keeping the design within the budget is a priority for the project. To keep the spending to a minimum, each part and mechanism went through a

process of evaluation; whether the part could be machined at the university's workshop rather than being purchased.

Weight is a factor that is related to the choice of material. For the upper part of the construction, aluminium is the preferred material which allows for maximization of applied load, by reducing the structural weight. As the density of aluminium is lower than steel, aluminium weighs less. Steel, on the other hand, was supplied on parts closer to the base of the Stewart platform. Parts made in steel weigh more and will therefore lower the centre of gravity for the construction when utilized on parts close to the base.

The Stewart platform's intended use is for research and exhibition at WNUAS. Thus, the design needs to look presentable, functional and reliable. As a result, keeping the design as simple as possible was a priority. Hence, the parts became easier to dimension and the finite element analysis (FEA) was easier to apply. A simple design uses the least amount of parts. Due to simplicity, a safer and more reliable design has been created as fewer connections have to be analysed using FEA. An exceeding number of connections ultimately leads to a higher risk of failure. Too many connections in a complex structure will force ANSYS to create multiple assumptions when running an analysis. This is integrated into the software to account for long-lasting process time and will lead to less precise results.

### 2.2.3 Dimensioning

The key component for the Stewart platform was the linear actuators. After debating between a hydraulic- or electric-driven system in Section 2.2.1, the choice fell on electric linear actuators. Afterwards, the wave data in Section 2.1.2 had to be interpreted and processed. The data displayed in Figure 4b indicated the speed range the simulation should be capable of replicating. These values became a key parameter when searching for an optimal type of actuator.

Another major parameter for choosing the correct actuator was the stroke length. Stroke length is a measurement of the linear displacement of the actuator. Figure 5a in Section 2.1.2 gave the largest distance from minimum to maximum, which was 250 mm. Adding the results from equation (6), as the actuators operate at an angle, forces an increased stroke length of maximum 280 mm. After defining each parameter, a list of the requirements for the actuators is shown in Table 2 below. Safety factor, as specified in the requirement list, is also critical to have in mind throughout the whole design process, as this needs to be considered in every decision.

| Requirements for the actuator |
|---|
| 300 mm stroke |
| Minimum speed of around 150 mm/s |
| 60kg load capacity |
| Stepper motor |

Table 2: Linear actuator requirement list.

## 2.3 Source of errors

There were many possible sources of errors which could affect the project. A great portion of the project had to be based upon data from former projects [8]. The former projects also included a source of errors like anchoring, placements, and geometry of the test object. As this project was based upon these data, the former project's errors were transferred to this project.

Another source of error was that the actuators would most likely not run exactly as the parameters written in the technical data discussed later in Section 3.1.7, which describes the actuators in-depth. The actuators can run wave simulations with a great margin. Therefore, the small errors transferred from technical data to reality will not play a major role in running simulations.

FEA is a method for numerical solutions of equations. Complex models can be created, where errors usually occur when simplifying these models. In addition, singularity errors and errors which can arise while generating mesh are also common while using this method.

# 3 Results

Throughout this project, a considerable number of various results have been collected. Based on these results, regarding design and construction, individual solutions which fit each result have been drawn. As this is a development project, the whole process is presented from start to finish. From the design of each part, ANSYS simulations, and to the complete assembled construction.

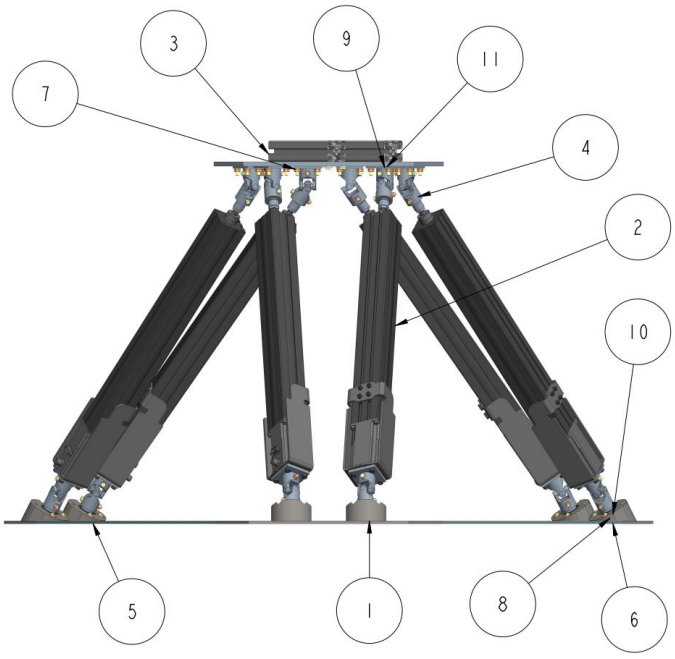


Figure 8: Visual overview.

| No. | Main component | Quantity |
|---|---|---|
| 1 | Bearing housing assembly | 6 |
| 2 | Actuator assembly | 6 |
| 3 | Platform assembly | 1 |
| 4 | Top-joint assembly | 6 |
| 5 | Base | 1 |
| 6 | M6x20 | 24 |
| 7 | M6x25 | 24 |
| 8 | M6 washer | 48 |
| 9 | M6x20 | 4 |
| 10 | M6 | 48 |
| 11 | M6 washer | 4 |

Table 3: List of components.

## 3.1 Parts and equipment

To ensure the Stewart platform's functionality, various parts are manufactured while others are ordered. Different equipment is used to assemble the structure and for machining different parts. In the following section, results are presented for each individual part from the fully assembled model.

### 3.1.1 Base

For the base of the structure, a steel sheet is acquired, as weight on the lower section of the structure is desired. The sheet is cut from a 1250x1250 mm profiled sheet into a hexagon shape with a diameter of 1100 mm, as seen in Figure 9.

The cutting was performed using a plasma table at the workshop. The plasma table operates using a computer. The 3D parts in Creo Parametric must be converted into STEP-files for the computer to read the files into its software. Holes larger than 10 mm will not be cut out by the plasma table. Holes which are smaller than 10 mm are marked at the centre. Therefore, the holes have to be manually drilled. The process starts by drilling a 6 mm hole in the centre of the mark using a bench pillar drill machine. Afterwards, the holes are drilled conical using a 12 mm counterbore.

Placing heavy objects on the platform could cause the Stewart platform to start shaking and tilting. A decision was made to compensate with a solid base that enables the possibility of placing heavy sandbags on the steel sheet. While running simulations with heavy objects on top, the sandbags create a lower centre of gravity. Lower centre of gravity results in a more stable structure. Reducing the thickness of the sheet and using a plasma table to produce shapes which use less material than the hexagon is therefore unnecessary. Some thickness is also a necessity when drilling counterbores.

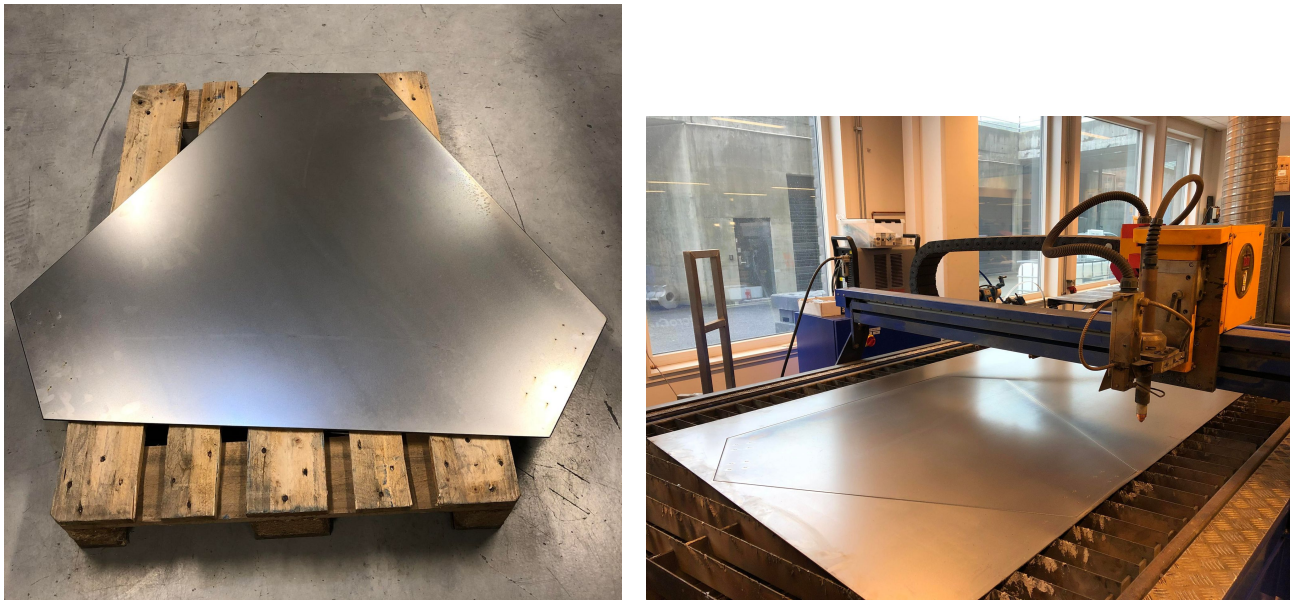

(a) Base on a Euro pallet.

(b) Base on plasma table.

Figure 9: Base of the Stewart platform.

The base consists of four boltholes for each leg. As the bolts are placed from underneath the base, countersink holes are made to the side of the sheet facing the floor. This is to ensure that the bottom side is flush and therefore smoother to place on either the floor or a pallet.

The planned base was a 5 mm thick steel sheet. Due to delivery problems, the 5 mm sheet had to be replaced with a 3 mm sheet. The delivery date was far beyond the hand-in date for the project. The purchased countersink bolts are not applicable with a 3 mm sheet. Therefore, temporary steel sheets covering each bolted section were welded on top of the base. The extra sheets provide extra thickness, allowing the use of the purchased countersink bolts. Note that this could be a temporary solution until a 5 mm steel sheet can be ordered. The grey coating was applied to avoid rusting of the steel sheet. Figure 10 displays the coated sheet with brackets.

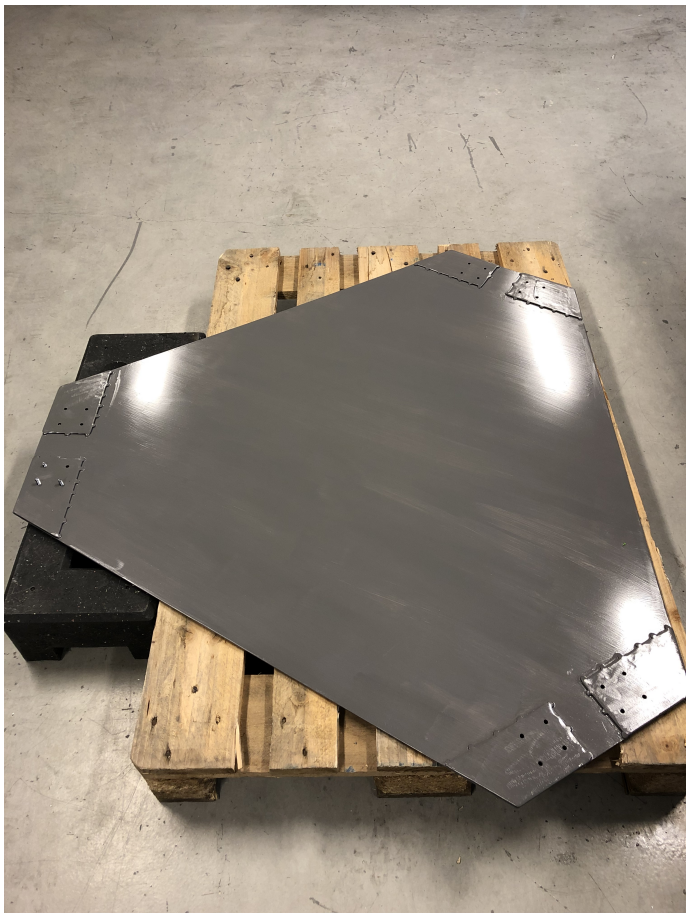

Figure 10: Coated base with brackets.

### 3.1.2 Platform

A 450x450 mm profiled aluminium sheet is supplied by the university to use as a platform and has a thickness of 8 mm. The platform has a smaller diameter of 300 mm but has the same hexagon shape as the base. As seen in Figure 11, two tracks in the middle of the platform are carved out. The tracks are a vital part of the adjustable fastening method, which enables objects with various bases to be bolted tight on the platform. This will be discussed in the next Sections 3.1.3 and 3.1.4.

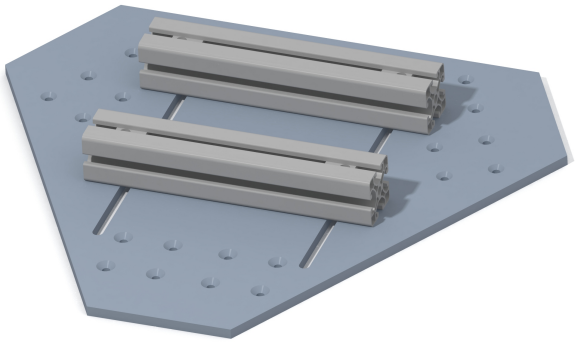

(a) Platform viewed in Creo.

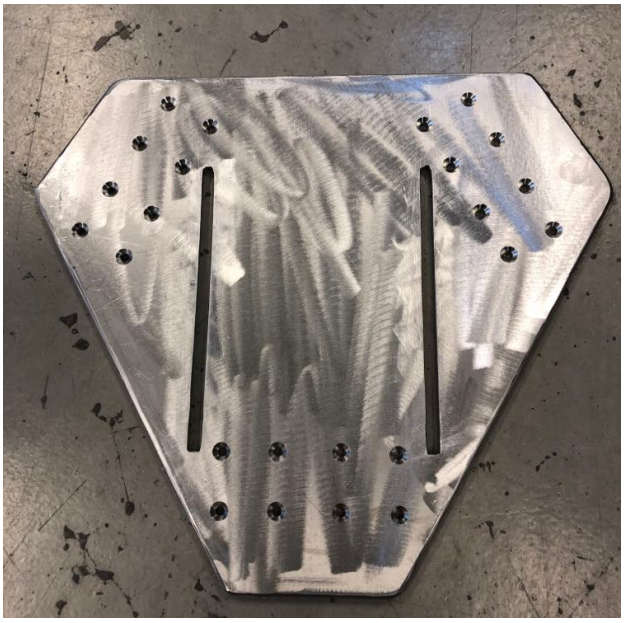

(b) Platform.

Figure 11: Platform displayed.

As illustrated in Figure 12, several design ideas were evaluated. Instead of having a solid aluminium sheet, the idea of creating an Aluflex structure was tested. The different designs will be further discussed in Section 4.1.1.

(a) Aluflex sketch no. 1.

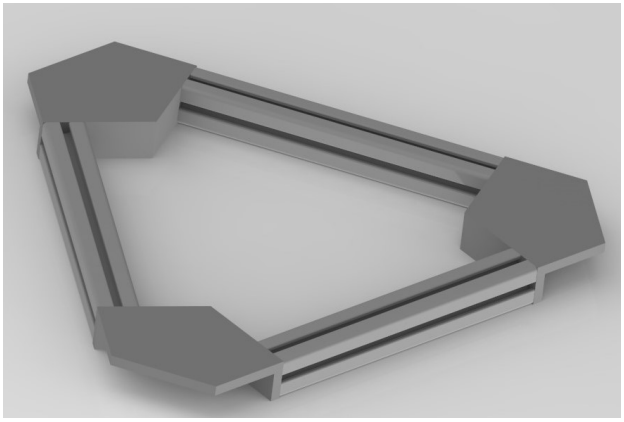

(b) Aluflex sketch no. 2.

Figure 12: Two different platform sketches.

The plasma table in the workshop is used for cutting out the platform from a large aluminium sheet. In addition, the plasma table cut out the tracks on the platform, both seen in Figure 13a. The same procedure as described in Section 3.1.1 applies for cutting out the base and drilling countersink holes for the platform. However, the tracks, despite having a diameter of 8 mm, are cut out by the plasma table.

The platform also consists of four boltholes for each leg, as described for the base. The platform and the base both use countersink holes, but the platform has holes on the top side while the base has holes on the bottom side. Using countersink bolts combined with Aluflex maximizes the total area use of the platform. With the platform surface being completely flush, which is seen in Figure 13b, almost the entire area can be utilized for attaching objects.

(a) Platform on plasma table.

(b) Countersink holes on platform.

Figure 13: Plasma table and countersink holes.

### 3.1.3 Aluflex

Two Aluflex parts are used on the top of the platform to tightly fasten the simulated object. Aluflex allows for adjustments in different directions. One direction of movement is along the Aluflex tracks, displayed in Figure 14a. The distance between them can be modified. Bolts fasten the Aluflex from underneath the platform, which makes the platform available for objects with various bases and bolt patterns. The Aluflex profile used is 40x40 mm and is cut out to be 220 mm long. In addition, Aluflex is available at the university, which leads to less spending from the budget.

There are custom-made slides which fit in the tracks of the Aluflex. The slides combined with the tracks create a high level of adjustability when it comes to fastening objects to the platform. There are two slides on each Aluflex with M8 bolts and washers, where one is displayed in Figure 14b below.

(a) Two pieces with tracks displayed.

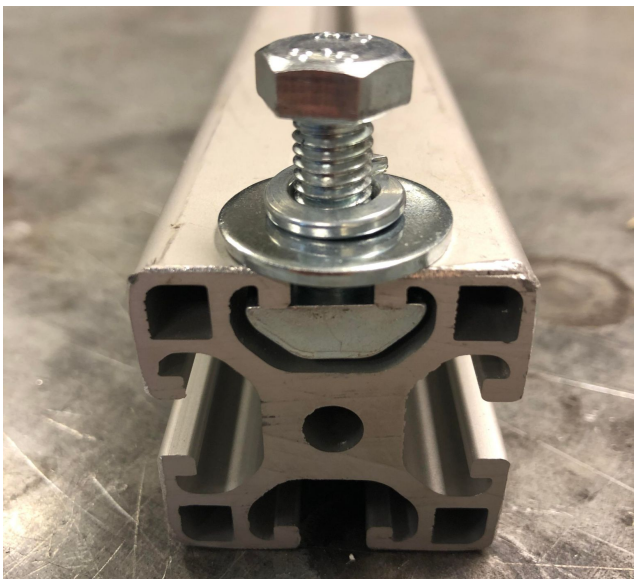

(b) Slides in the tracks.

Figure 14: Aluflex.

### 3.1.4 Adjustable fastening method

An adjustable fastening method is a requirement for the Stewart platform, as test objects vary in size and shape. The tracks combined with Aluflex are utilized to attach objects in different locations on the platform. A crane in various positions is displayed in Figure 15, where the adjustable fastening method shows its effectiveness.

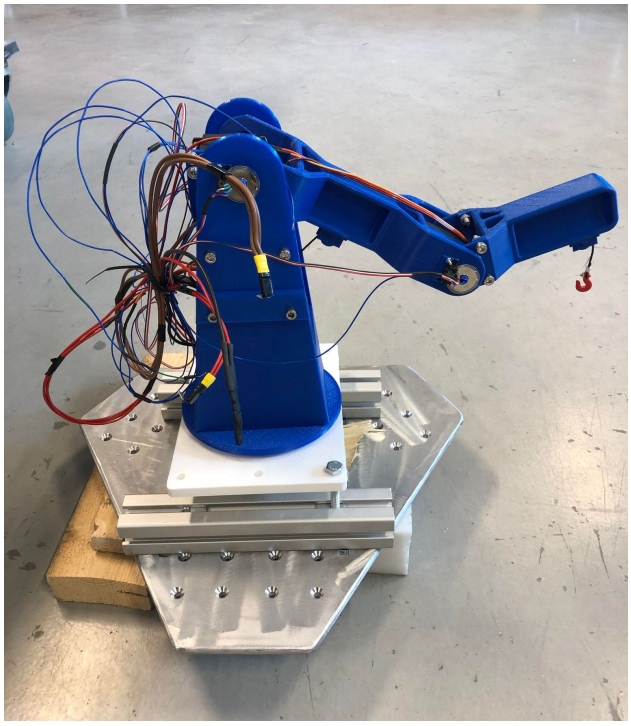

(a) Middle position.

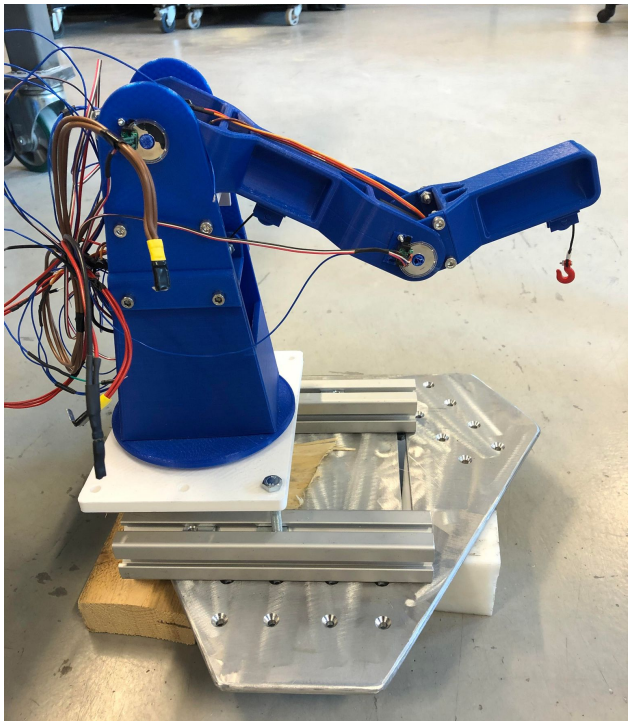

(b) Left position.

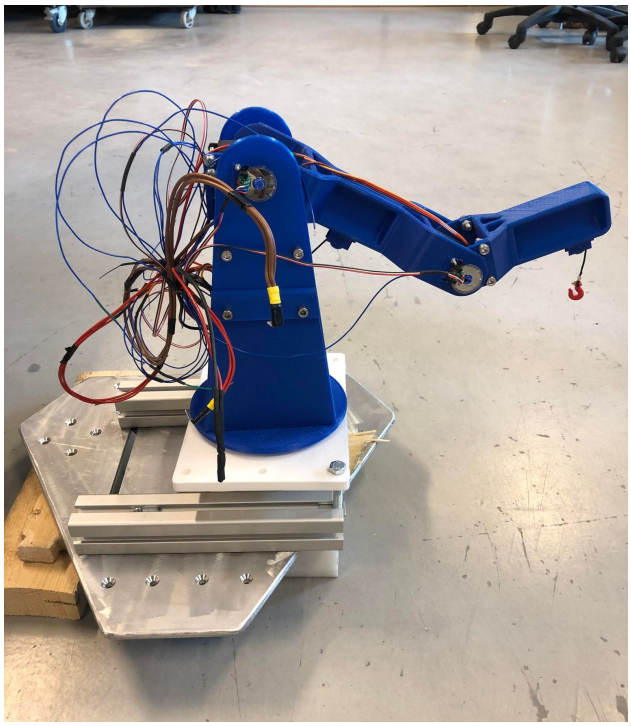

(c) Right position.

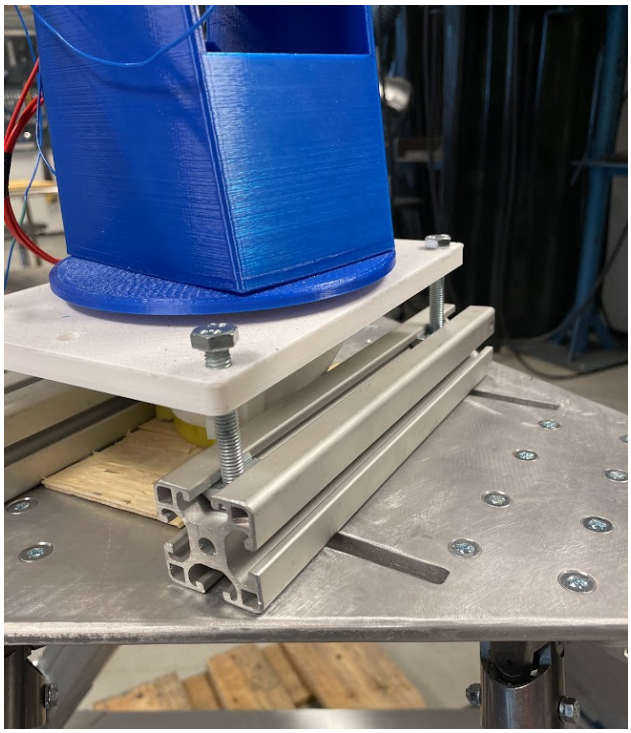

(d) Base of test-object connected to Aluflex.

Figure 15: Adjustable fastening method.

### 3.1.5 Joints and shafts

Twelve universal joints are purchased to acquire the desired DOF. Universal joints have two degrees of freedom. The method of attachment is to slide a shaft into both ends of the joint. The bore of the holes in each end is 16 mm. Due to the hole basis system, the shafts are milled with a 16 mm diameter using tolerances. The tolerances can be seen below in Table 4.

Pins are used as a locking mechanism between the shaft and joint. Pins exclude bending moment, which simplifies calculations in ANSYS. The joints were not initially equipped with pinholes when purchased. Drilling holes for pins are done manually at the University's workshop. The holes have a diameter of 5 mm in the upper section, and 6 mm in the lower section. The reason for hole variation has been described at the end of the current section. A jig was designed by hand at the workshop, which simplified the drilling of each of the 24 holes.

Figure 16: Universal joint with pinhole.

Three different shafts are machined at the workshop. Each of the shafts contains separate properties. All three shafts can be seen in Figure 17 below.

(a) Shaft with notch.

(b) Part that fits into bearing.

(c) Milled part.

Figure 17: Shafts.

Shaft (a) is produced with a notch. The reason behind the notch is to create a weak spot. The notch has a diameter of 8 mm in comparison to the 20 mm shaft external diameter. The actuators are already designed with a weak spot. The material selected for shaft (a), needed to have lower tensile strength than the material on the actuator. Designing shaft (a) with a smaller diameter and selecting a weaker material, ensures that the shaft breaks before the actuator's weak spot in the case of overload. The actuators are the most expensive components for this project and would be costly to replace. An M10x1.25 female thread is also carved out at the workshop to attach the shaft to the actuator. The other end has a drilled hole of 5 mm, which locks the position using a pin.

Shaft (b) is fitted into the bearing. To fit the shaft into the bearing, tolerances are applied when machining the shaft. A locational interference fit, $H^7/ p^6$, is machined around the shaft. The tolerance ranging from 0.0 mm to +0.021 mm made sure the shaft would not slip out of the bearing. A hole of 5 mm is also drilled into the shaft to attach it to the universal joint using a pin.

Shaft (c) is milled out of a block of aluminium. Thus, the shaft only consists of one end which is inserted into the universal joint. The block is attached in two different places on each leg. To the under-body of the platform and strictly underneath the actuators. This is visualized later in Section 3.3. The shaft is machined in a CNC milling machine, while shaft (a) and (b) is machined in a lathe.

The joint ends have the same dimensions and tolerances for all shafts. All three have a locational transition fit, which is tolerance $H^7/ n^6$. The tolerance ranges from 0.0 mm to +0.018 mm.

| **Shaft** | **Joint end [mm]** | **Tolerance [mm]** | **Opposite end [mm]** | **Tolerance [mm]** |
|---|---|---|---|---|
| **(a)** | 16.0 | +0.018<br>0.0 | 20.0 | (Threaded) |
| **(b)** | 16.0 | +0.018<br>0.0 | 20.0 | +0.021<br>0.0 |
| **(c)** | 16.0 | +0.018<br>0.0 | - | - |

Table 4: Shaft dimensions [10].

Shaft (c) consists of two variants. The original milled shaft, which is equal to the drawing in Appendix A, has a thickness of 6 mm at the square section. The other has a thickness of 14 mm. The thick shafts are used in the lower section of the Stewart platform, while the thinner shafts are connected to the platform. All shafts originally had the same thickness, but after assembling shaft (c) to the platform, the purchased countersink bolts came up too short. As a result, six segments of shaft (c) are cut to the original thickness using the CNC machine.

The pinhole on the shaft also endured a variation. Instead of using a 5 mm pinhole, the pinhole turned out to be 6 mm from the CNC machine. Hence, the universal joints have an upper pinhole of 5 mm and a lower pinhole of 6 mm. The variations were caused by miscommunication between the group and the CNC machine operator.

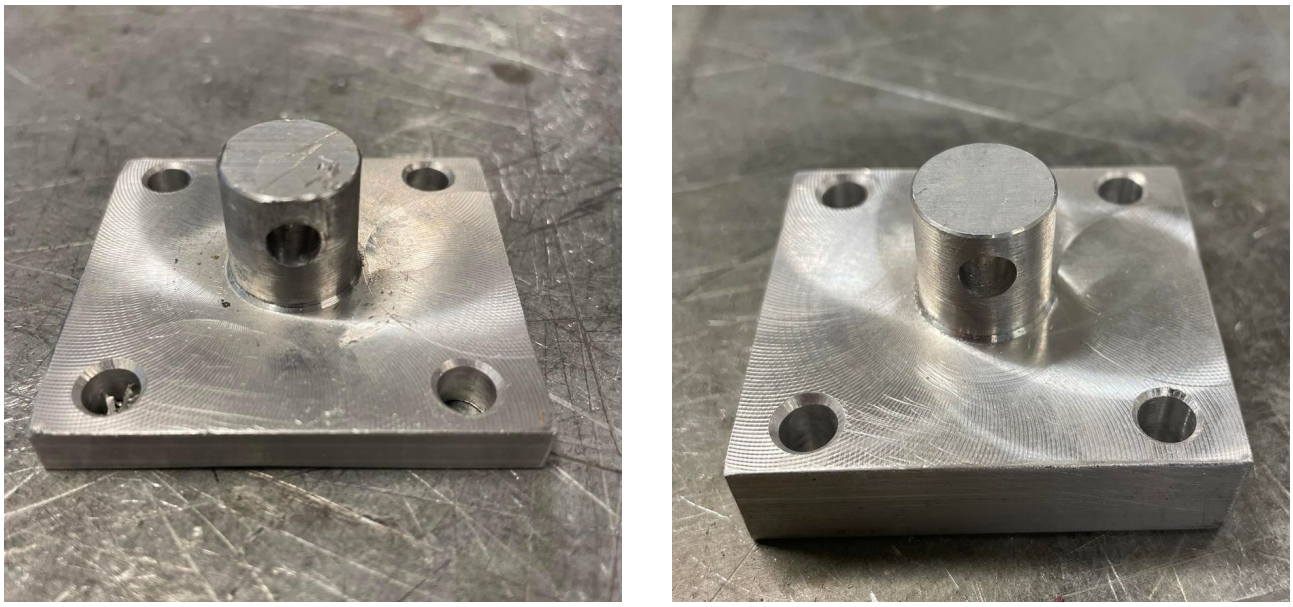

(a) 6 mm.

(b) 14 mm.

Figure 18: Thickness variation.

### 3.1.6 Bearing and -housing

The key role of the bearings is to generate an additional degree of freedom for the construction. Bearings provide the last degree of freedom in the lower section as the six actuator legs are required to rotate. The maximum load on the platform is 60 kg, which means the bearings are not required to withstand a high static load. The selected bearing can however withstand a static load of 2.96 kN [11]. The dimensions selected have an inner diameter of 20 mm, which fits the machined shaft. An outer diameter of 37 mm matches the designed attachment method.

The reason for selecting the current bearing, is that the dimensions fit the rest of the components. Almost each of the available bearings at the supplier could withstand the applied forces listed above with a great margin. A seal is also included, which means the bearings do not require external grease. Hence, low maintenance.

– 6x RS PRO Deep Groove Ball Bearing - Plain Race Type, 20mm I.D, 37mm O.D

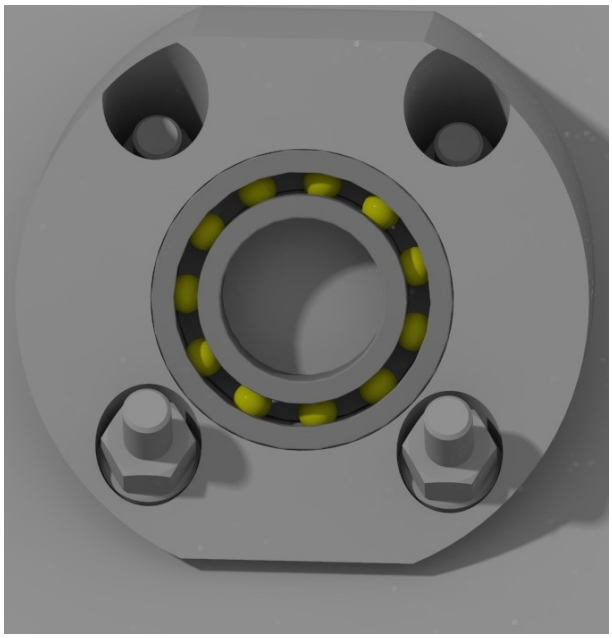

(a) Bearing housing with bearing viewed in Creo.

(b) Bearing.

Figure 19: Bearing housing with bearing in Creo and bearing in reality.

A bearing housing is designed to fit the bearing. The bearing housing is produced using Polyoxymethylene (POM). POM is a thermoplastic material with high strength and hardness [12]. The housing started as a cylinder of POM, before being inserted into the lathe for further processing. The lathe cut out a fit for the bearing and a penetrating hole in the centre of the fit. A locational interference fit is used to fit the bearing into the housing. Shaft basis $P^7/ h^6$ has a tolerance of -0.008 mm. When the hole basis is cut out, the bearing is forced into the locational interference fit. Work done by the lathe is visualized in Figure 20a.

First, the CNC machine flattens out each side of the housing. Flat surfaces allow the part to be locked to the vice in the CNC machine. Furthermore, the work continues by extruding boltholes for attaching

the housing to the base. The boltholes in the housing have two different extrudes. The first extruded bolthole is 6 mm. To fit corresponding nuts to the 6 mm bolts, a second extrusion was needed. The second extrude had a hole diameter of 17.32 mm. Work done by the CNC machine is displayed in Figure 20b.

(a) Lathe.

(b) CNC machine.

Figure 20: Work done by different machinery.

A final design of the assembled bearing including the shaft is displayed below in Figure 21.

Figure 21: Bearing housing.

### 3.1.7 Actuator

The selection of this type of electric linear actuator with a stepper motor is a result of the previously analysed data from Section 2.1.2 and the budget described in Section 2.2.1. As the values correspond with the requirement list from Table 2, EPCO-40-300-5P-ST-E is ordered. A visual representation is shown below in Figure 22.

– 6x Festo EPCO-40-300-5P-ST-E

Figure 22: EPCO-40-300-5P-ST-E.

An overview over technical data is viewed in Figure 23.

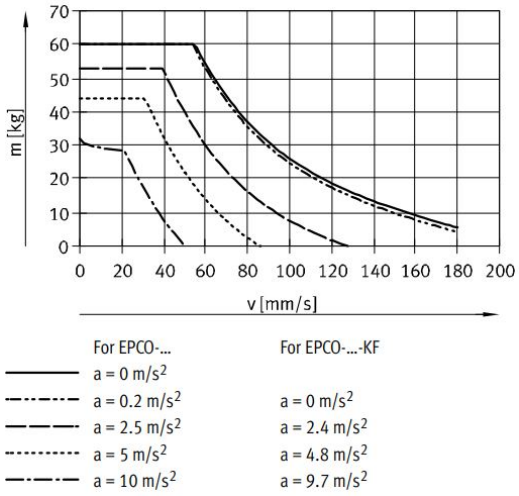


(a) Mass as a function of speed and acceleration [13].

| Feature | Value |
|---|---|
| Stroke | 300 mm |
| Spindle diameter | 12 mm |
| Assembly position | Any |
| Piston-rod end | Male thread |
| Motor type | Stepper motor |
| Max. Acceleration | 10 m/s2 |
| Max speed | 0.18 m/s |
| Duty cycle | 100% |
| Nominal operating voltage DC | 24 V |
| Nominal current | 4.2 A |
| Reference value for working load, horizontal | 120 kg |
| Reference value for working load, vertical | 60 kg |

(b) Key technical data [14].

Figure 23: Technical data.

Accelerations from the wave data sets are another analysed parameter. Comparing wave data accelerations to values the actuators holds, the data become insignificant due to the large value differences. Figure 23a shows data from the actuators where the acceleration values are much higher than the analysed parameters from the wave data. As a result, the acceleration data has not been provided with an in-depth analysis.

The decision of using a stepper motor instead of a servo motor fell to both price, availability, and the expertise of the project's supervisor. The world is currently in a microchip shortage [15]. The

situation is impacting everyone, including this project, making suitable controllers hard to obtain. Using a servo motor requires a servo drive, which had a delivery time of almost a full year. The price is also significantly higher. Stepper motors are cheaper and still capable of performing within the project's specifications. The responsibility for selecting the controllers are shared with the supervisor to make sure the post-project software integration is feasible. Corresponding parts such as cables and mounting kits were found, which is displayed in Section 3.1.9.

### 3.1.8 Bolts and nuts

Bolts and nuts are used as the preferred connection method. Adding additional washers allows parts to be easily assembled, and if necessary, replaced. Welding was up for debate and will be discussed further in Section 4.1.2.

Bolt dimensions are listed here:

- M5: Locks the shaft and lower part of the universal joint using a locking pin
- M6: Connects the shaft and upper part of the universal joint using a locking pin
- M6 (countersink): Used for connecting platform and base to each actuator leg
- M8: Used to fasten objects to the Aluflex

Figure 24: M5 and M6 countersink with nuts and washers.

### 3.1.9 Adapter kit, motor- and encoder cable

An adapter kit is necessary as it enables vertical mounting of the actuator. It also gives additional support. As the actuator is the most expensive part of the construction, the extra support from the kit helps. The motor- and encoder cables are needed to control the motion of the Stewart platform. Since the control system engineering is not a part of this thesis, a detailed description of the cables is therefore not relevant.

- 6x EAHA-P1-40 (Adapter kit)
- 6x NEBM-S1G9-E-2.5-Q5-LE6 (Motor cable)
- 6x NEBM-M12G8-E-2.5-LE8 (Encoder cable)

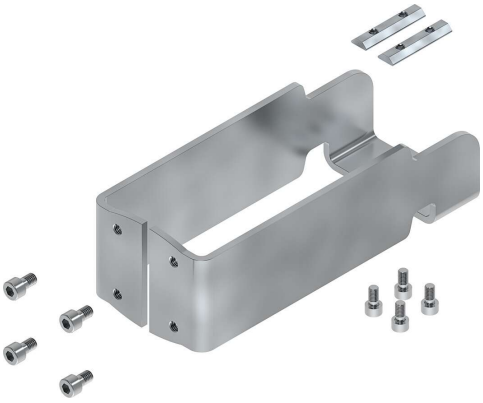

Figure 25: Adapter kit [16].

## 3.2 Results - using ANSYS

Finite Element Analysis ensures that every part of the construction will withstand the applied forces and not exceed maximum strength limits. Some deformation will always appear, but selecting a material with suitable properties can reduce this. Most of the different parts are simulated in ANSYS using reaction forces to locate the most fragile spots in the construction. Simulations are conducted with a maximum force of 1200 N, which accounts for a safety factor of two for the load. The simulations are set to calculate the stress (Von Mises) and total deformation that appear in each part. Boundary conditions are applied to each of the parts in ANSYS. These are also displayed throughout this section.

The upper- and lower part of the joint attachment, seen in Figure 26, are identical. The simulation shown below is analysed using the maximum forces. Therefore, only one analysis has been shown, despite that they are used at two different locations in the construction. The joint attachment uses bolts to connect with the platform for the upper part, and actuators for the lower part. Fixed support is applied in the four bolt holes while a force is pulling downward on the pin-connected shaft with an angle.

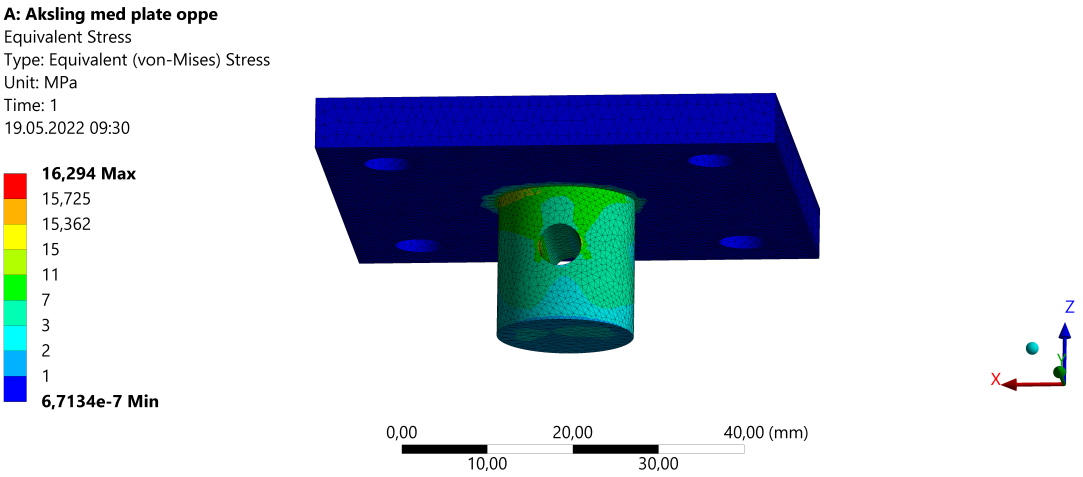


(a) Stress (Von Mises).

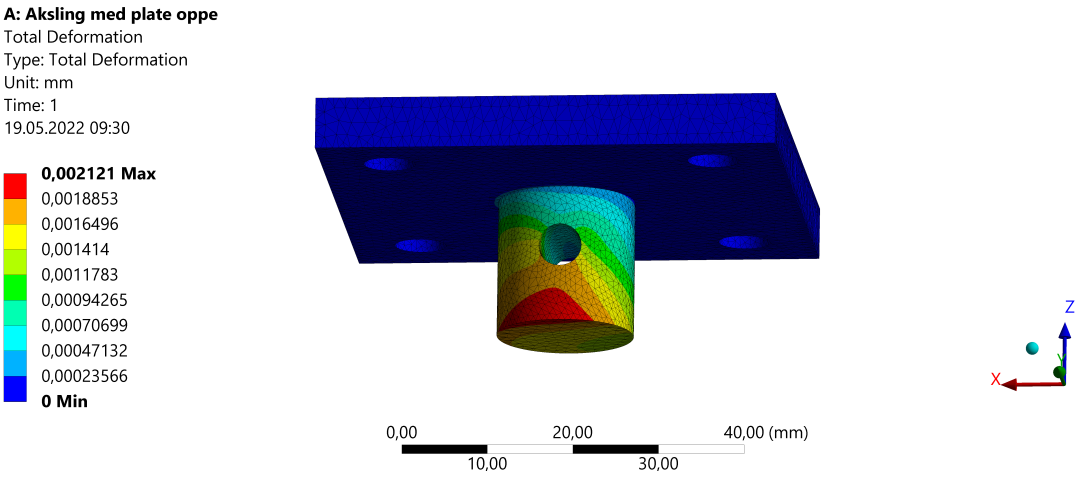


(b) Deformation.

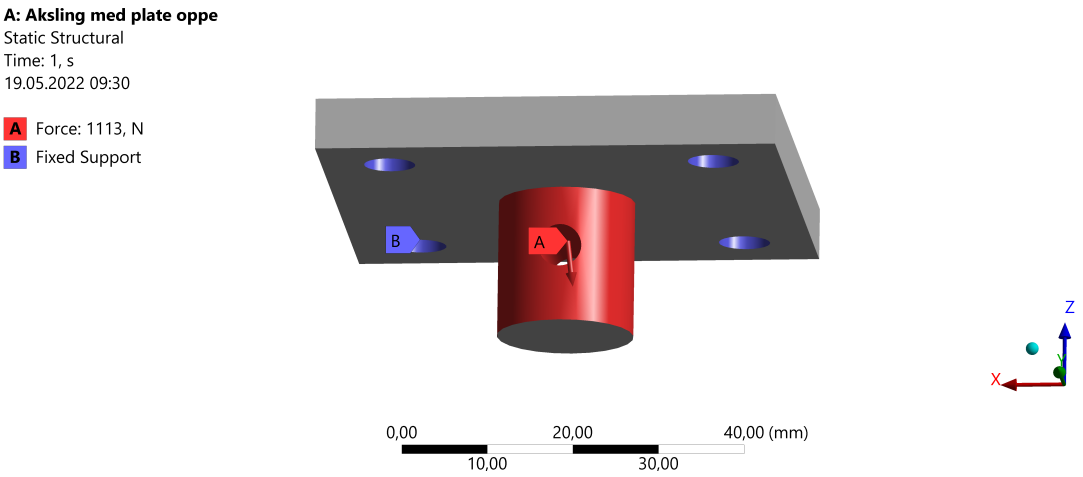


(c) Boundary conditions.

Figure 26: Upper- and lower part of joint attachment, aluminium.

The shaft in Figure 27 is connecting the universal joint to the top of the actuators. This part is designed with a notch, a weak spot, as it is easy to replace and can be produced at the university. The highest stress appears in the desired place, hence; the part withstands the required load. Deformation is minimal for this part.

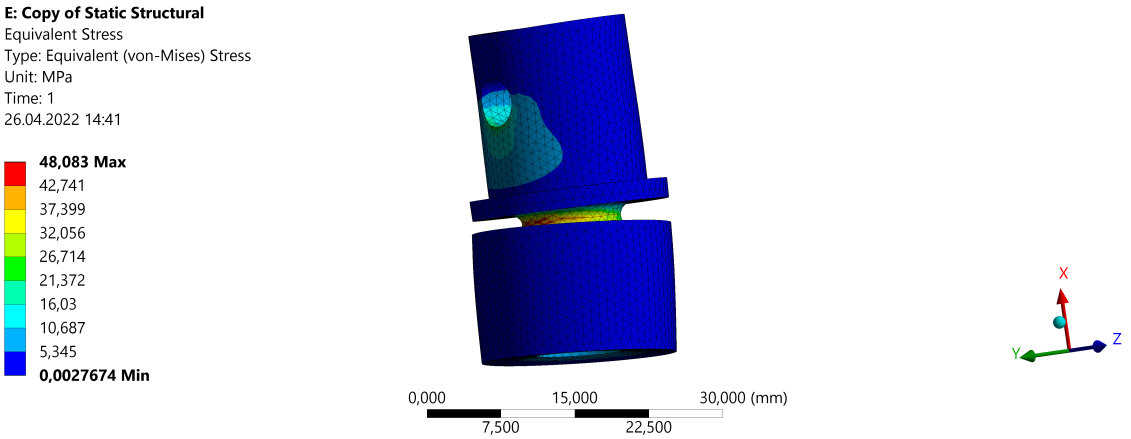


(a) Stress (Von Mises).

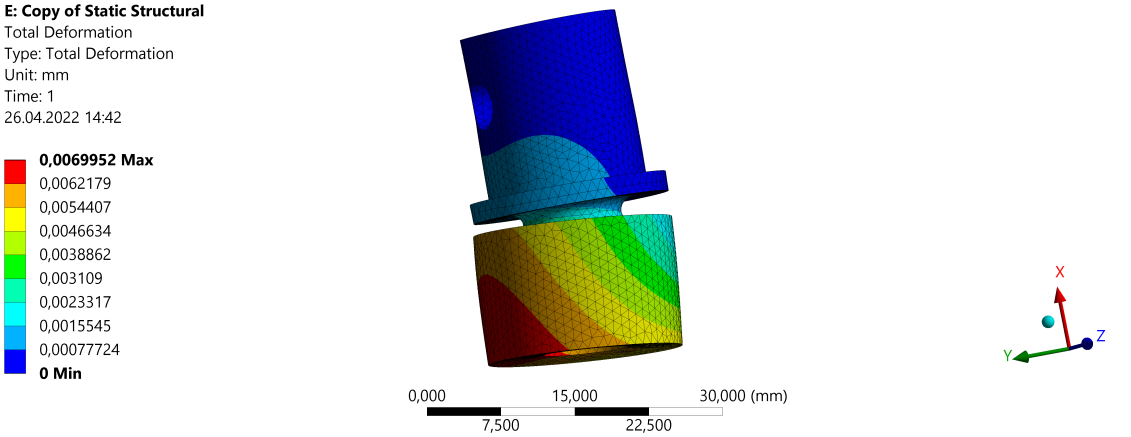


(b) Deformation.

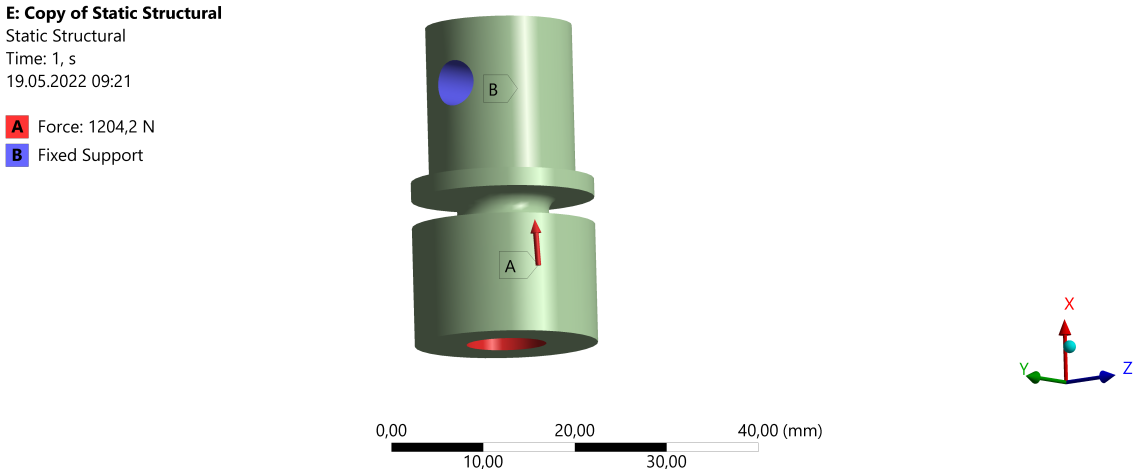


(c) Boundary conditions.

Figure 27: Weak-spot part of joint attachment, aluminium.

Universal joints are mechanisms used in two different locations on each leg. The analysis in Figure 28 is performed using the maximum force of 1200 N. Stresses that appear in the joint are well below the maximum tensile strength regarding the selected type of steel. The deformation of the universal joint is also very small.

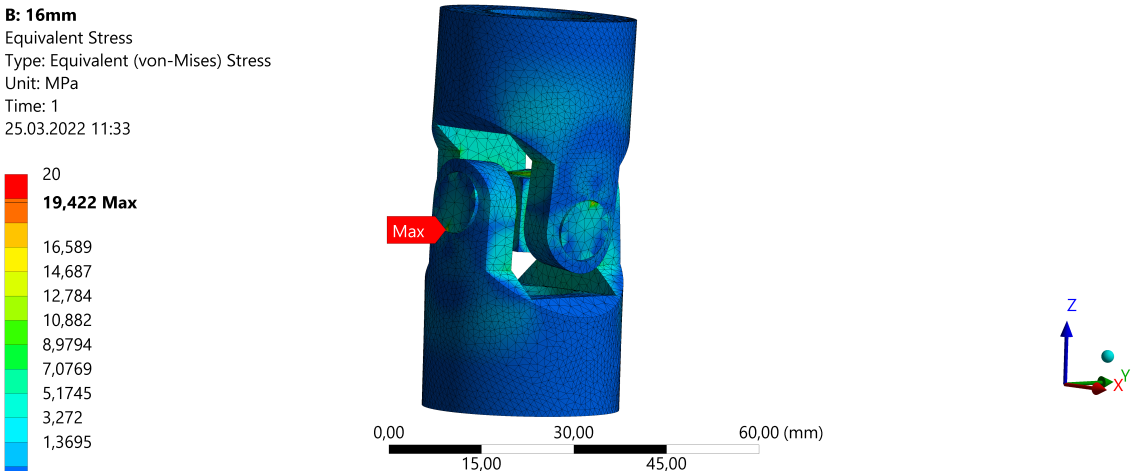


(a) Stress (Von Mises).

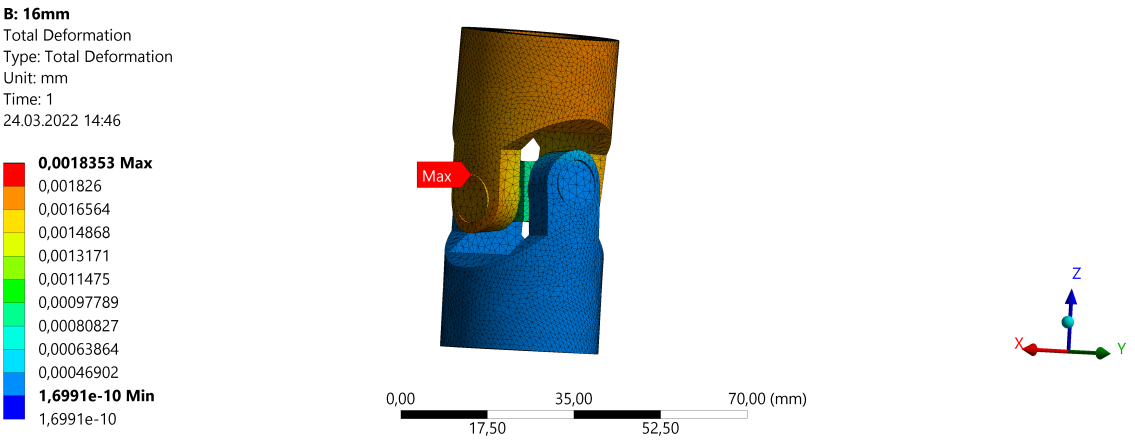


(b) Deformation.

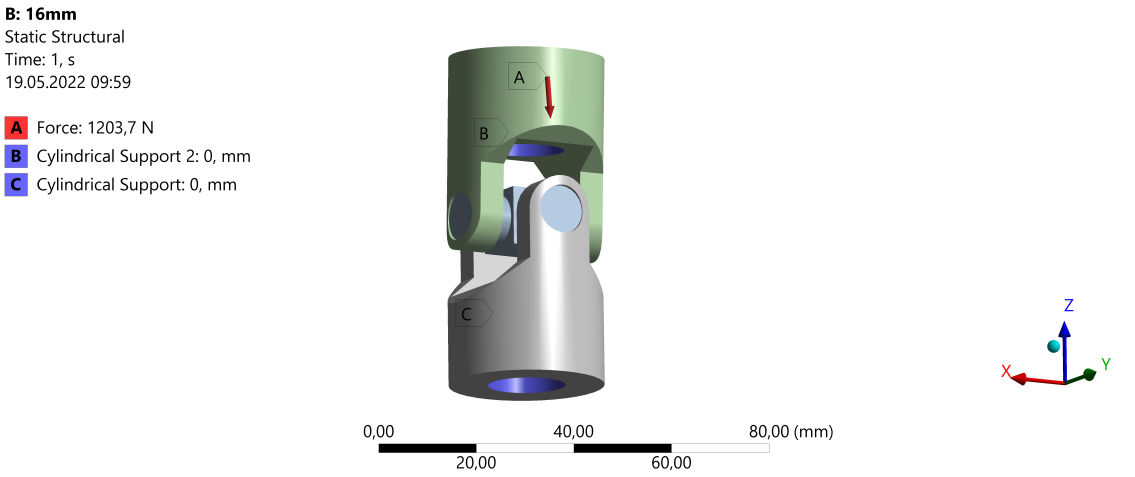


(c) Boundary conditions.

Figure 28: Universal joint, steel.

Figure 29 shows the part that connects the pinned universal joint and the bearing. The simulation is performed using a force on the pin and the surface where the joint rests. Fixed support is used on the shaft on the bottom of the part. As seen, the level of deformation and stresses are at a minimum.

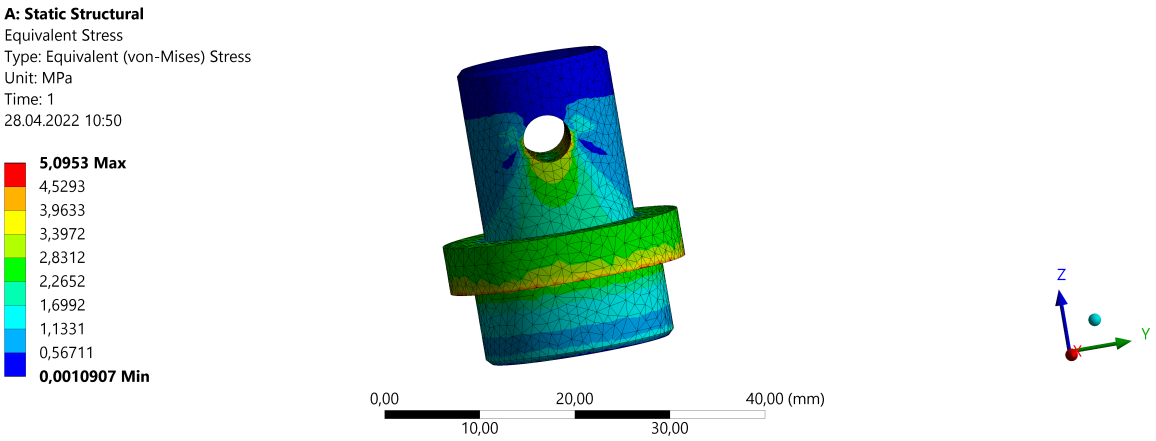


(a) Stress (Von Mises).

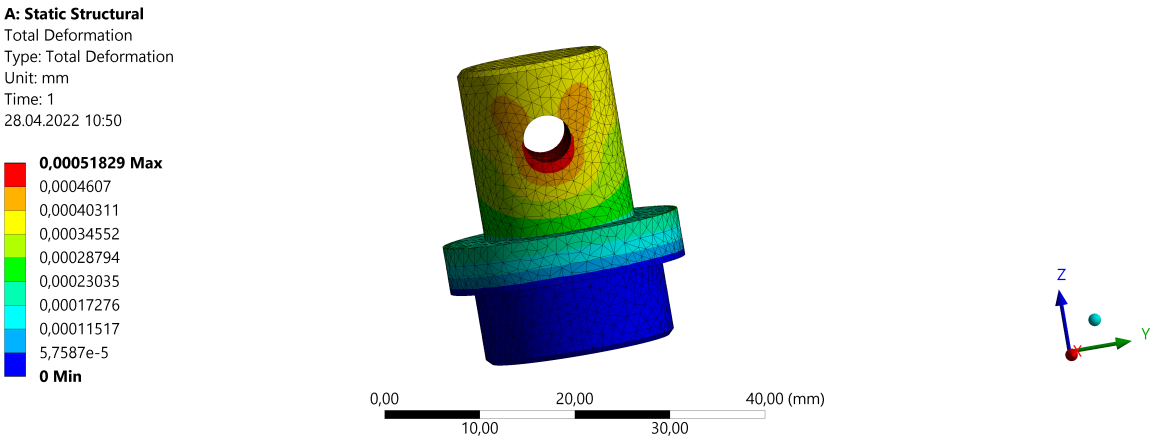


(b) Deformation.

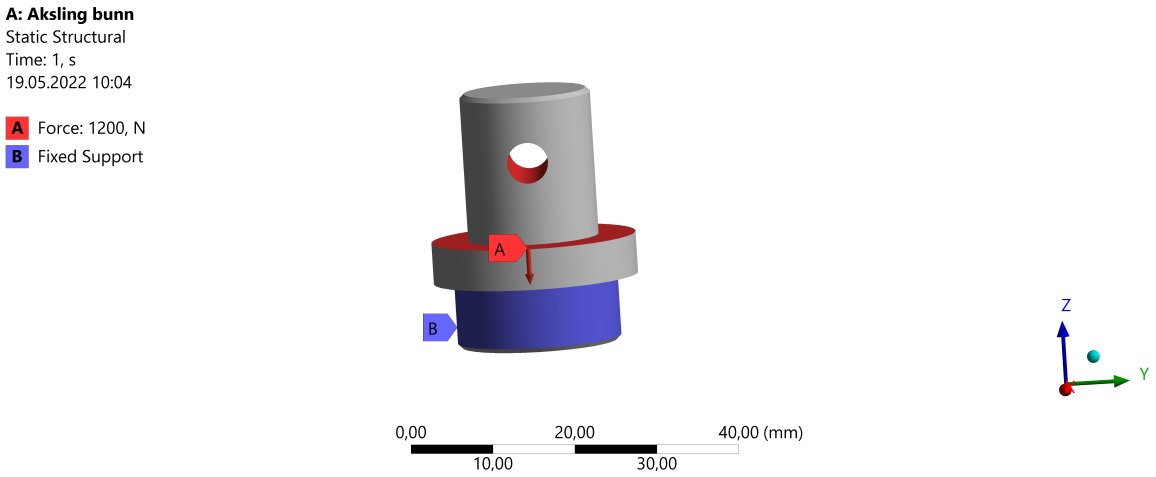


(c) Boundary conditions.

Figure 29: Shaft with pin, aluminium.

Figure 30 displays the bearing housing which is connected to the base of the Stewart platform. The bearing housing is made using POM. The properties of this material were already implemented in the ANSYS library. Looking at the deformations and stresses which appear on the bearing housing, these are well within the maximum tensile strength of the material properties. The deformation is also minimal.

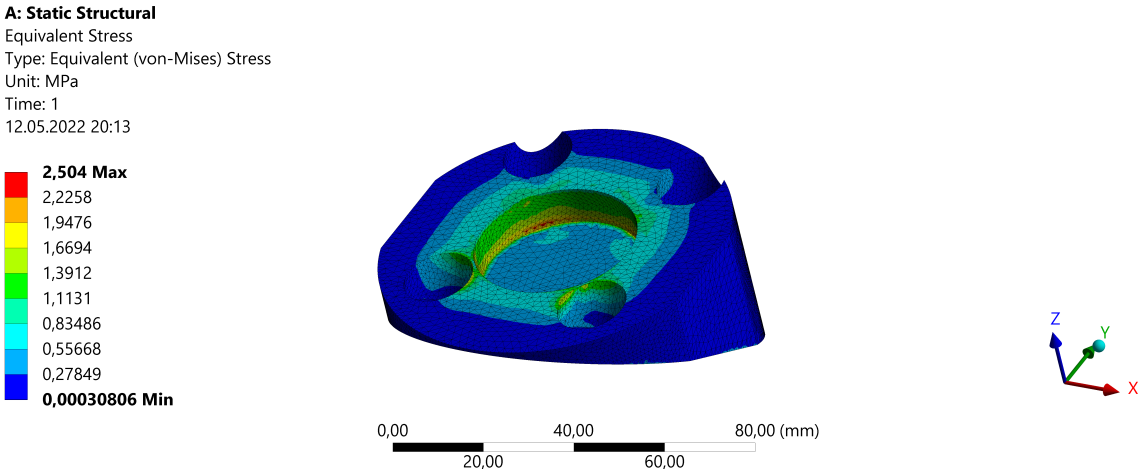


(a) Stress (Von Mises).

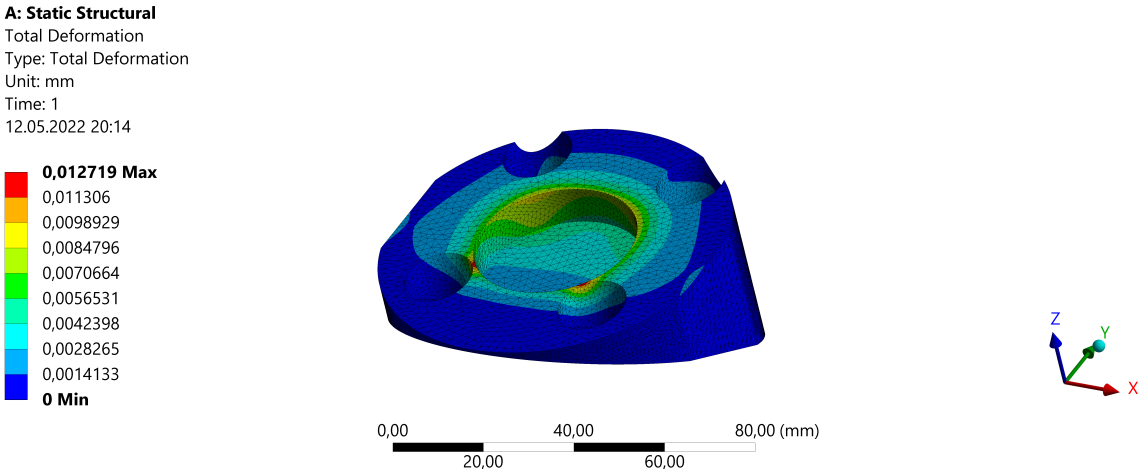


(b) Deformation.

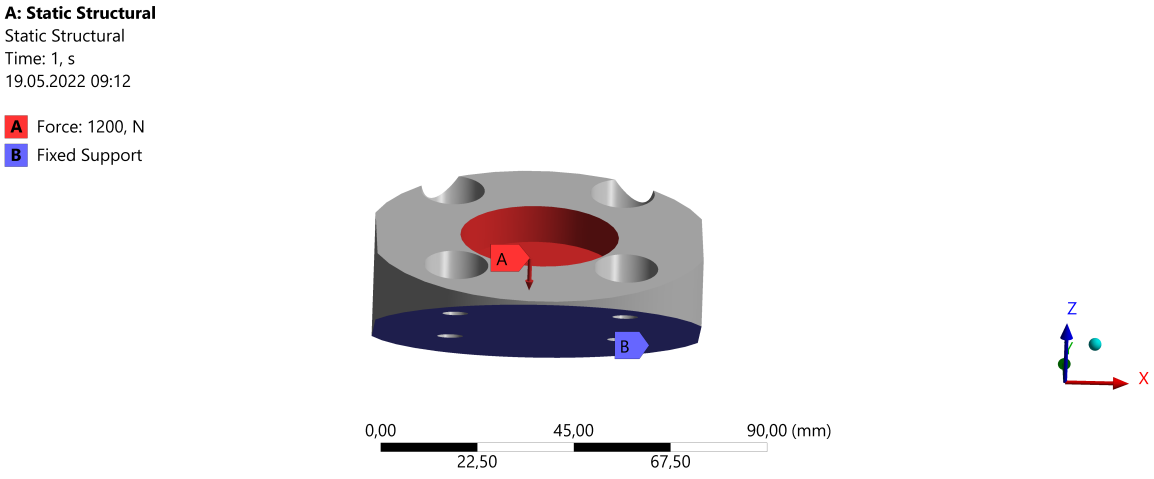


(c) Boundary conditions.

Figure 30: Bearing housing, POM.

Figure 31 displays simulations when five of the six actuators are locked in place, while the remaining actuator accelerates with full force. These maximum forces could appear on the platform. Hence, the aluminium block from Figure 26 is fastened with four bolts under each of the boltholes where deformation happens. This was taken into account in the design process and therefore supports the platform. The deformation is already quite small but will be even smaller when the construction is assembled because of this support.

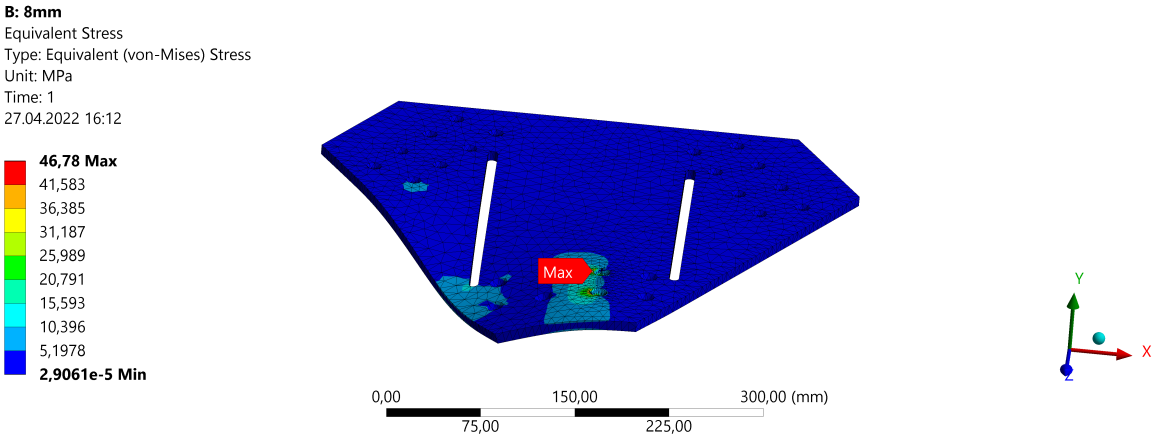


(a) Stress (Von Mises).

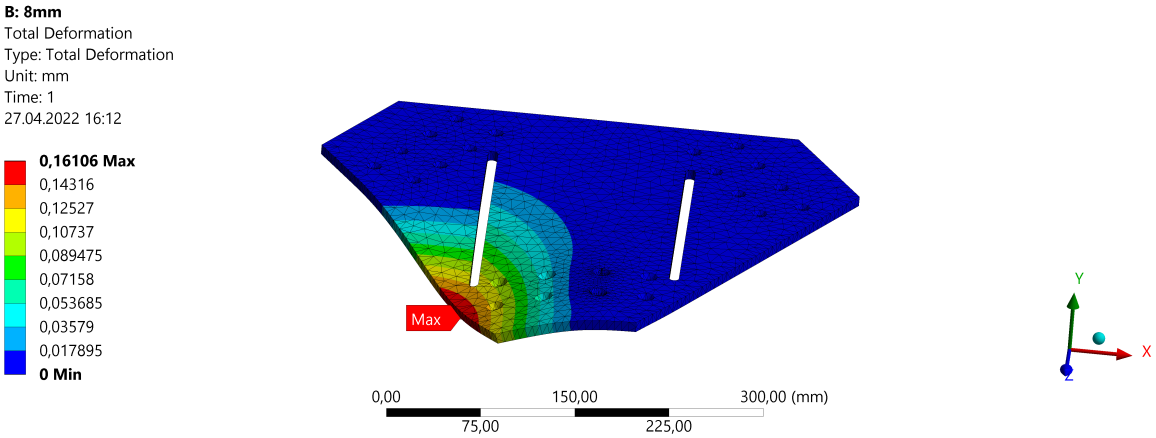


(b) Deformation.

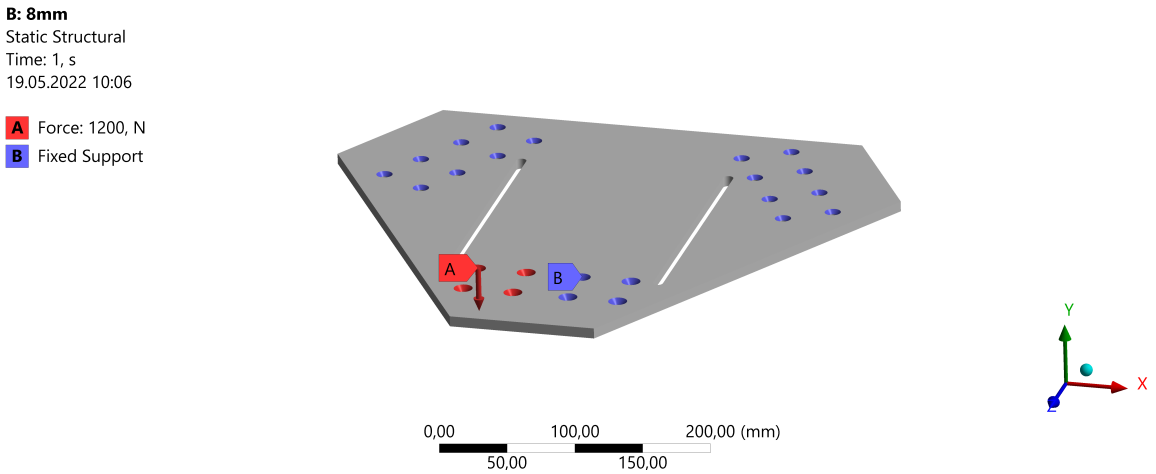


(c) Boundary conditions.

Figure 31: Platform, aluminium.

## 3.3 Construction

The connections between all parts of the Stewart platform uses either bolts, nuts, washers and locking discs or different types of fits. Both the machined parts and shorted bolts are grinded to produce round edges. Every part has been described throughout the thesis. The remaining part of the result is to assemble and construct the Stewart platform. The construction is seen in Figure 32 below.

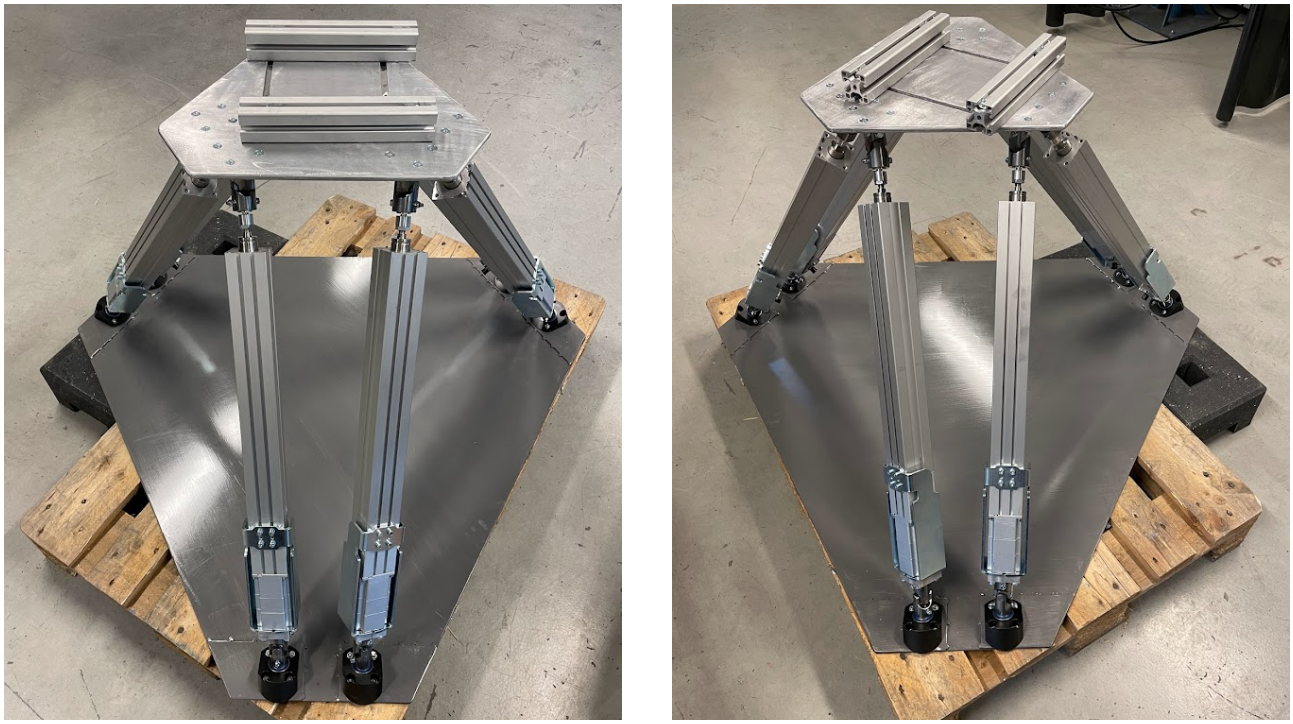

(a) View 1.

(b) View 2.

Figure 32: Fully constructed Stewart platform.

An assembly of the legs are displayed in Figure 33 and visually describes the process starting from the bottom, up to the top.

The base is at the bottom, preferably placed on a pallet or the floor. Angled bearing housings are connected to the base using four countersink bolts and nuts for each leg. An exploded view of the assembly of the lower part of the leg can be seen in Figure 33a. Bearings are fitted into each of the bearing housings, while a shaft is fitted using a locational interference fit into the bearings. Universal joints slide into the other end, applying a pinned-locking mechanism. On the other end of the joint, the milled part of aluminium slides into the joint while fastening them using pins. Bolts connect this part onto the actuators with the help of their corresponding adapter kits. The shaft with a notch is threaded to the shaft of the actuators, which again slides into the universal joints and fastened with bolted pin connections. The exploded view of the upper part of the assembly is displayed in Figure 33b. On the other end of the joints are the milled part, which slides into the joints and is locked with a bolt. Finally, the platform is connected to the milled part using countersink bolts, placed from the platform's topside, and nuts. Two Aluflex pieces are fastened on the tracks of the platform, using bolts, washers and custom made slides.

The figure below displays a realistic visualization of the leg-assembly in contrast to using CAD software.

(a) Lower part of the assembly.

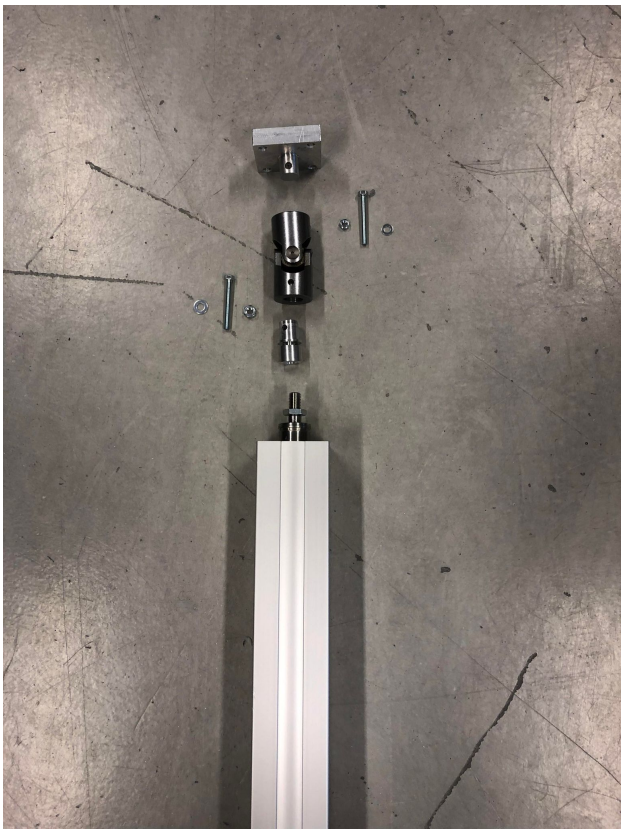

(b) Upper part of the assembly.

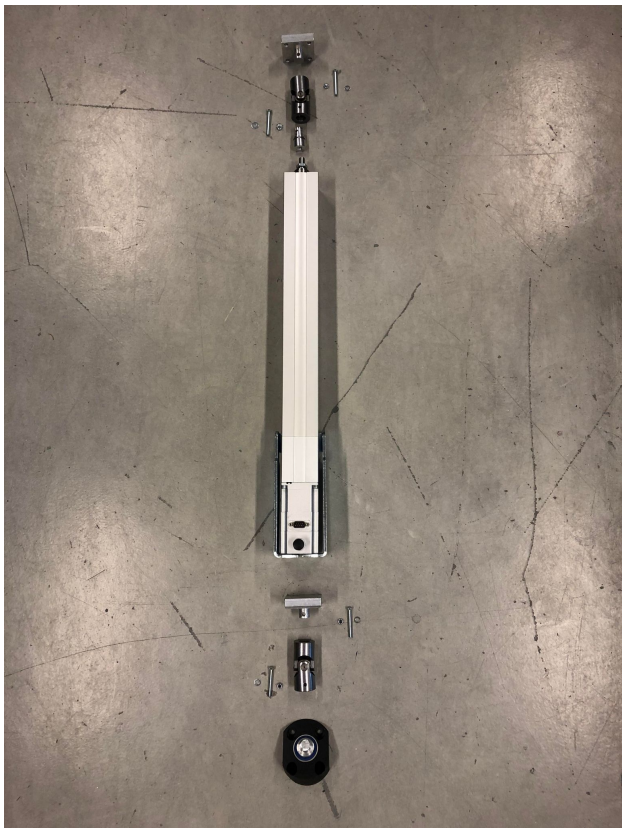

(c) Whole leg assembly.

(d) Fully assembled leg.

Figure 33: Leg explode and assembly.

## 3.4 Total cost

Table 5 below, displays an overview of the total cost of the project. The project's total cost comes at 87 275,19 NOK. The table also includes control system components. From the available budget, a total of 112 724,81 NOK is remaining. Cost efficiency was defined as a primary objective at the start of the project. The table shows that the objective has been completed.

| **Component** | **Quantity** | **Price [NOK]** |
|---|---|---|
| Actuator w/ motor | 6 | 7 757,00 |
| Motor cable | 6 | 566,00 |
| Encoder cable | 6 | 498,00 |
| Adapter kit | 6 | 467,00 |
| Micro controller | 6 | 240,86 |
| Stepper motor controller | 6 | 2 649,32 |
| Power supply 24V | 3 | 1 514,00 |
| Power supply 12V | 2 | 1 589,44 |
| Power cable Arduino | 6 | 81,24 |
| Power extension cord | 1 | - |
| Power cable - two conductors | 1 | - |
| Bearing | 6 | 116,67 |
| Bearing housings | 6 | - |
| Bearing shaft | 6 | - |
| Universal joint | 12 | 441,67 |
| Milled shaft | 12 | - |
| Notch shaft | 6 | - |
| Aluflex | 2 | - |
| Aluflex attachment | 4 | - |
| M6 countersink bolt w/ nut | 48 | - |
| M6 bolt w/ washer | 4 | - |
| M5 bolt w/ nut | 24 | - |
| Platform (8 mm, aluminium) | 1 | - |
| Base (5 mm, steel) | 1 | - |
| **Sum** | | **87 275,19** |

Table 5: Total cost of project.

Note: "-" means the component has been machined or covered by WNUAS.

# 4 Discussion

In the following section, several aspects of the thesis are discussed. This includes alternative solutions which have been considered and the selection of different materials, among else. The desired outcome of the project has been to design and construct a fully functional Stewart platform. As a result, decisions have been made based on various discoveries in different topics of discussion.

## 4.1 Design

Throughout the project, different drafts for designing the Stewart platform were considered. The flowchart in Figure 34, illustrates some of the different ideas for this project. Justifications for the choices made during the manufacturing process have been clarified earlier in the report and will be discussed deeper in the following section.

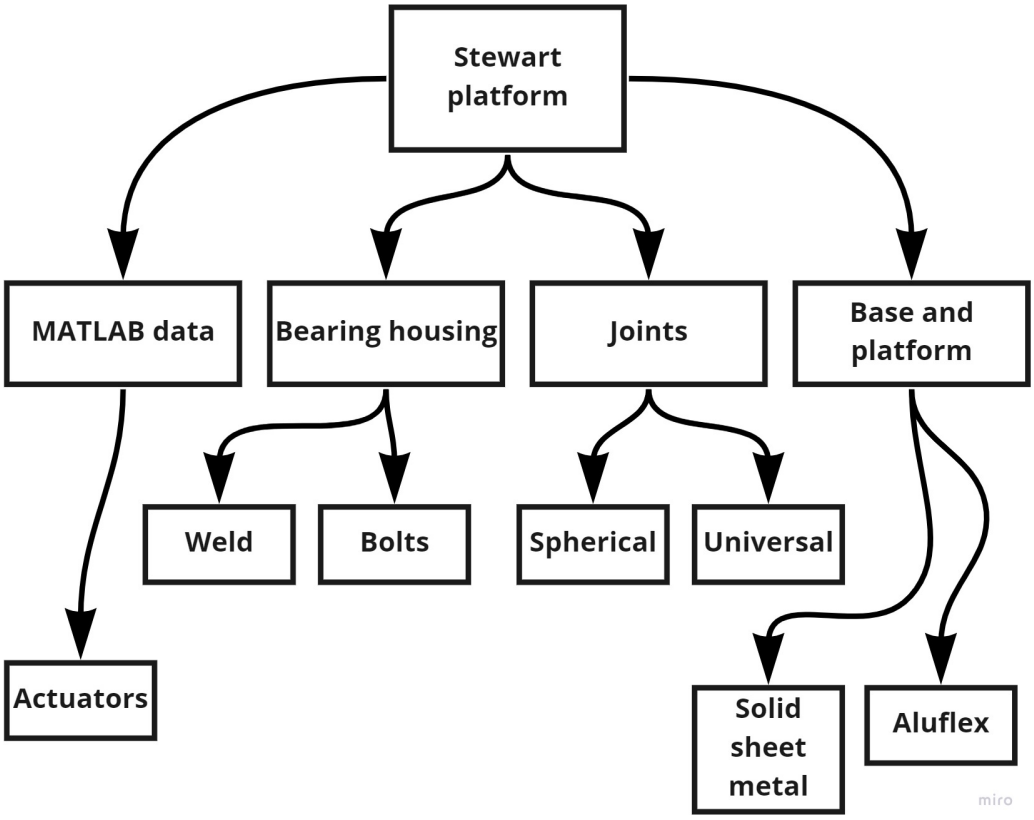


Figure 34: Flowchart of design alternatives.

### 4.1.1 Base and platform

The platform had three different sketches which are shown below in Figure 35. Two of them were built using Aluflex in the platform structure. The last one purely consisted of an aluminium sheet using Aluflex as the method of attachment.

Sketch 35b have angled brackets drilled into each end of the Aluflex beam. Connecting the platform to the joints underneath would require more points/surfaces which would make the design overcomplicated. A method of attaching on top of the platform would make the sketch even more complicated. As a result, the sketch got scrapped early in the process.

Sketch 35c has the same Aluflex-structure as Sketch 35b. The difference appears at each end of the Aluflex parts. Instead of bolting each end, an idea was to use welding. Bolting could also be used since it would increase simplicity and accuracy. The disadvantage in the sketch is the end-brackets. It would have required a vast amount of machining to manufacture the brackets.

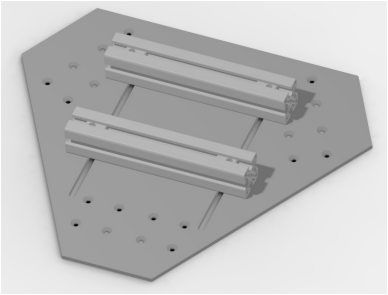

(a) Aluminium sheet.

(b) Aluflex no. 1.

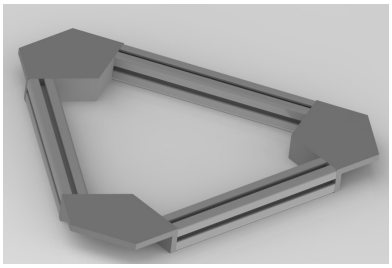

(c) Aluflex no. 2.

Figure 35: Three platform sketches.

An evaluation of each parameter in the separate sketches are shown below in Table 6. The scale varies from 1-3, where 3 is best and 1 is the poorest, and has been used to assess the best sketch.

| Sketch | Machining | Method of attaching | Assembly (weld, bolts etc.) | Connection to lower joints | Total score |
|---|---|---|---|---|---|
| **(a)** | 3 | 3 | 3 | 3 | **12** |
| **(b)** | 2 | 1 | 1 | 1 | **5** |
| **(c)** | 1 | 2 | 1 | 3 | **7** |

Table 6: Assessment of sketches.

As Table 6 displays from total score, Sketch 35a is selected. With respect to the production process, the Aluflex sketches did not come as far in the process to analyse stress and deformation.

A crane which is placed on the bow of a boat at sea will experience more motion than a crane that is placed in the middle. The same principles apply for the Stewart platform as well. Objects which are placed in the front of the Stewart platform will experience more motion than objects placed in the centre. Therefore, this design is selected.

### 4.1.2 Joints and method of attachment

Weld or bolts was considered for connecting the bearing housing to the base and the joint attachment to the platform. The platform's material is aluminium. An 8 mm aluminium sheet and weld would cause the aluminium to twist in varying directions and magnitudes. This inflicts precision and overall strength in the construction. Precision is required in this project to uphold certain angles and lengths.

Using bolts and nuts fits this project the most. The Stewart platform is going to be used in the future for lab exercises and research experiments. In that case, the platform may be modified for various reasons. Bolts make the platform easy to modify in the future.

Connecting the bearing housing to the base required another design concerning the upper joint attachment. An extra degree of freedom had to be acquired, which led to the use of bearings. In addition, the operating angle of the universal joint is between 3° and 45°. Therefore, the bearing housing has been raised to a 30° angle. An angled bearing housing allows the universal joint to operate at the desired operating angle. Using the designed solution leaves the total operating angle at 10°. This ensures that the universal joints do not exceed the maximum operating angle. The original idea used weld to raise the rectangular surface 30°. The idea has been illustrated with an early draft in Figure 36b. The blue- and orange coloured strip illustrates weld. After cooperating with the lab engineers, the decision was made to design a circular shape instead of rectangular and use bolts instead of welds. In Figure 36a the selected draft is displayed with bolts as a method of attachment.

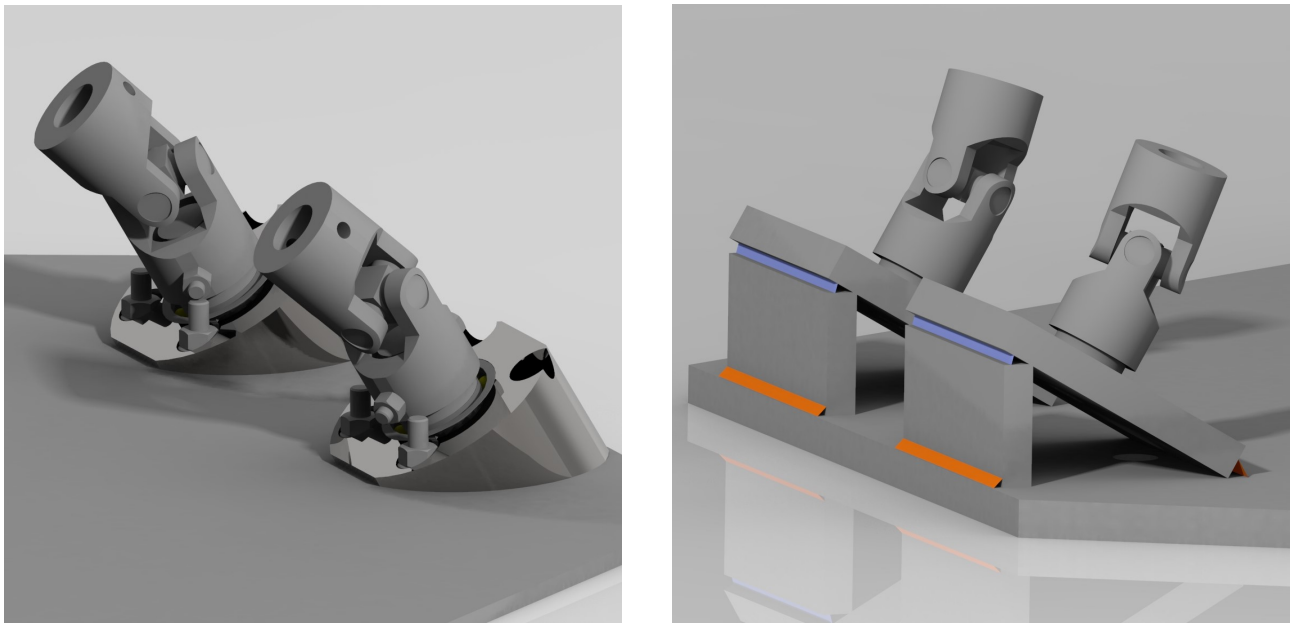

(a) Bolted. (b) Welded.

Figure 36: Drafts of different joint attachment.

To select the correct joints; universal- and spherical joints were considered. Available spherical joints were not found at any nearby suppliers. Spherical joints can operate using three DOF. Universal joints also transmit torque compared to spherical joints. This is solved using bearings. Universal joints were therefore selected.

## 4.2 ANSYS simulations

ANSYS simulations on the platform were performed using the maximum load of 1200 N. From there, the reaction forces were found at a certain angle. The centre of gravity varies and does not remain constantly in the centre of the structure. The platform was originally supposed to be 5 mm aluminium, but simulations showed that high deformations would appear. Based on these simulations, seen in Figure 37a, a decision was made to increase the thickness of the aluminium sheet to 8 mm instead. The Stewart platform is constructed to perform high-speed dynamical operations. This means that a high deformation would quickly lead to permanent deformations on the platform. As seen in Figure 37b, the deformation is far lower than on the previous 5 mm sheet.

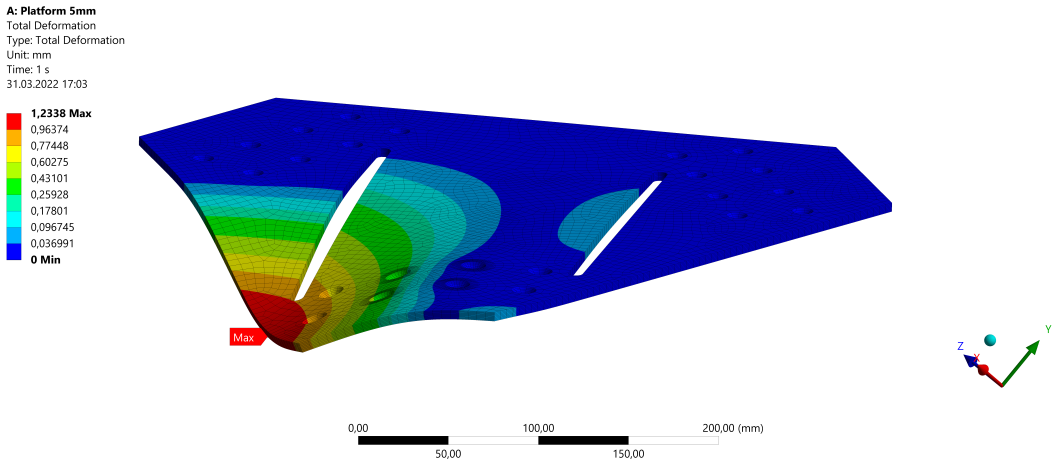


(a) 5 mm.

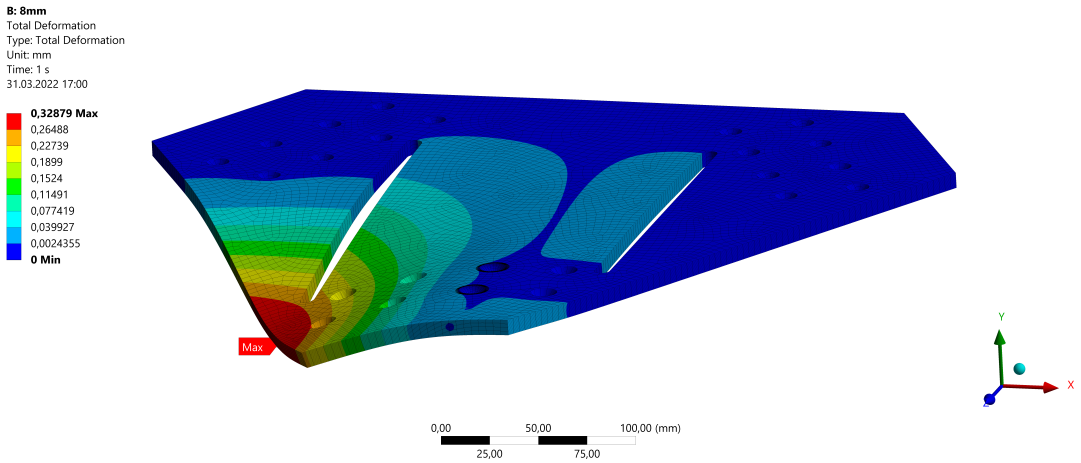


(b) 8 mm.

Figure 37: ANSYS results when thickness is increased.

## 4.3 Electric versus hydraulic

There was a desire for a hydraulic-driven system for the Stewart platform from the start of this project. As the budget described in Section 2.2.1, the cost for a hydraulic-driven system was higher than an electric system. Figure 38 shows how much higher the operation efficiency is using an electric linear actuator. Hydraulic systems require power when the system is in use to keep the system pressurized, resulting in inefficient use of power. On the other hand, electric actuators require none or very low current to keep their positions. In other words, the only time electric actuators need power is when they change positions, resulting in very efficient use of power [17]. Servo- and hydraulic systems also require more maintenance than electric systems. Therefore, electric actuators are mostly used on modern systems that will allow it. The decision was therefore made to use electric actuators instead of a hydraulic system.

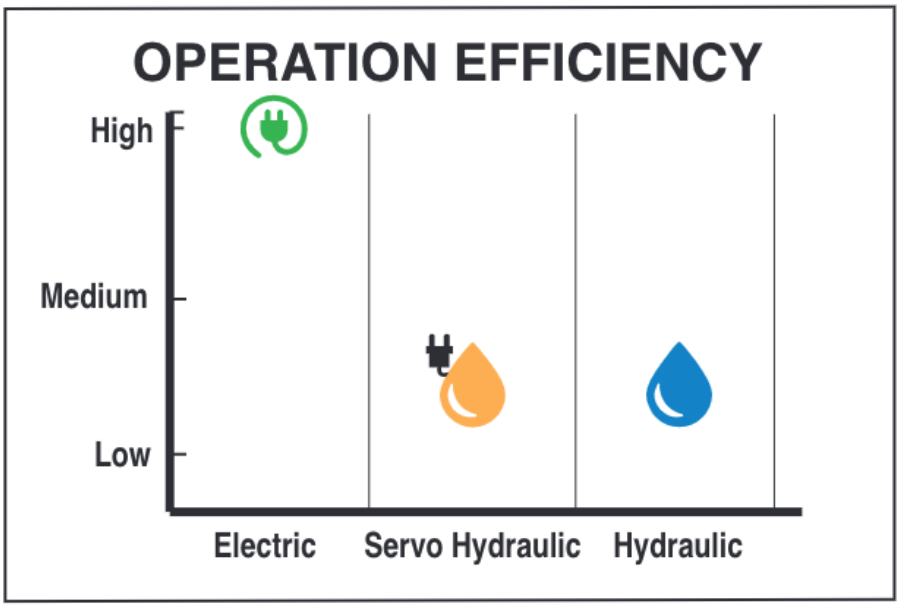


Figure 38: Operation efficiency using different actuators [17].

## 4.4 Materials

The selection of materials for the different parts is mainly based on three factors; strength, weight and availability. As every part is analysed through ANSYS, the forces which appear are accounted for and shall not exceed the maximum tensile strength for either of the selected materials.

Aluminium is mostly used on parts closer to the top, as less weight is desired on the upper part of the platform, while more weight is desired on the bottom part. This greatly reduces the risk of tilting while the Stewart platform operates on the border of its limitations. The base of the structure is a steel sheet, which has a higher density than aluminium and for that reason, weighs more. POM was the chosen material for the bearing housing since POM was available at the university. This comes back to an objective for the project, mentioned earlier, to use material from the university and therefore avoid unnecessary spending. The electric linear actuators are made using stainless steel and those are the only part of the Stewart platform that uses this type of material.

# 5 Conclusion

Concluding the entire thesis, an electric driven Stewart platform which fits on a Euro-pallet, and has six degrees of freedom was constructed. The Stewart platform enables a maximum load of 60 kg, including a factor of safety, tilts $\pm$ 25° for pitch and roll and allows for a yaw rotation of $\pm$ 40°. Finite element analysis has been performed on every necessary part of the assembled Stewart platform. Wave data has been interpreted and electric linear actuators have been carefully selected based on these measurements. The speed of the actuators enables the Stewart platform to operate with a high level of accuracy compared to the analysed wave data. An adjustable fastening method was designed which allows objects to be placed and fastened in various positions on the platform when running simulations. The fully constructed Stewart platform is seen in Figure 39 below.

For further work, the software and control system has to be written and developed, as this was not a part of the thesis. With the control of each stepper motor, the motion of the linear actuators can be operated. Combining each actuator's motion will allow for simulating different wave motions and complex movements.

Taking all this into account, the set requirements are fulfilled, and a fully functional Stewart platform has been designed and constructed. The Stewart platform will be used for developing, researching and testing different products and objects in the future.

(a) View 1.

(b) View 2.

Figure 39: Final product.

# References


[1] Flabio Dario Mirelez-Delgado, José Ronaldo Díaz-Paredes, and Miguel Abraham Gallardo-Carreón. Stewart-gough platform: Design and construction with a digital pid controller implementation. *Automation and Control*, 11 2020.

[2] D. Stewart. A platform with six degrees of freedom. *Proceedings of the Institution of Mechanical Engineers*, 180:371–386, 6 1965.

[3] PTC Creo.

[4] Ansys — Engineering Simulation Software.

[5] MathWorks - MATLAB & Simulink.

[6] Dag Ingvar Jacobsen. *Hvordan gjennomføre undersøkelser?* Cappelen Damm Akademisk, 3 edition, 2016.

[7] Roy de Winter. 3.4: Roll, pitch, yaw, heave, sway, surge of a ship. — download scientific diagram. *Researchgate*, 5 2018.

[8] Jørgen Fjøsne, Håvard Gjøsaeter, and Trym Telle. Miniatyrsensor for bølgemåling-effekten av bølger og oppankring på bøye. Bachelor's thesis, Western Norway University of Applied Sciences, 2017.

[9] Magnus Berthelsen Kjelland, Morten Ottestad, Geir Hovland, and Michael Rygaard Hansen. Design of a heave compensation system with a redundant hydraulic manipulator. Master's thesis, University of Agder, 2011.

[10] Pat Rapp. *ENGINGEERS Black Book (metric)*. Pat Rapp Enterprises, 3 edition, 2018.

[11] RS Components. SS61904-2RS — RS PRO Deep Groove Ball Bearing - Plain Race Type, 20mm I.D, 37mm O.D — RS Components, 2022.

[12] C. V. Pious and Sabu Thomas. Polymeric materials-structure, properties, and applications. *Printing on Polymers: Fundamentals and Applications*, pages 21–39, 9 2015.

[13] Festo. Electric cylinders EPCO, with spindle drive, 2021.

[14] Festo. electric drive EPCO-40-300-5P-ST-E, 2022.

[15] Tom Linton and Bindiya Vakil. Why we're in the midst of a global semiconductor shortage. *Harvard Business Review*, 2021.

[16] Festo. Adapter kit EAHA-P1-40 — Festo EE, 2022.

[17] Aaron Dietrich. Electric rod actuators vs. hydraulic cylinders: A comparison of the pros and cons of each technology, 2016. Approved by author.

# List of Figures

# List of Tables

# Appendix

## Appendix A: CAD Drawing

### Complete assembly

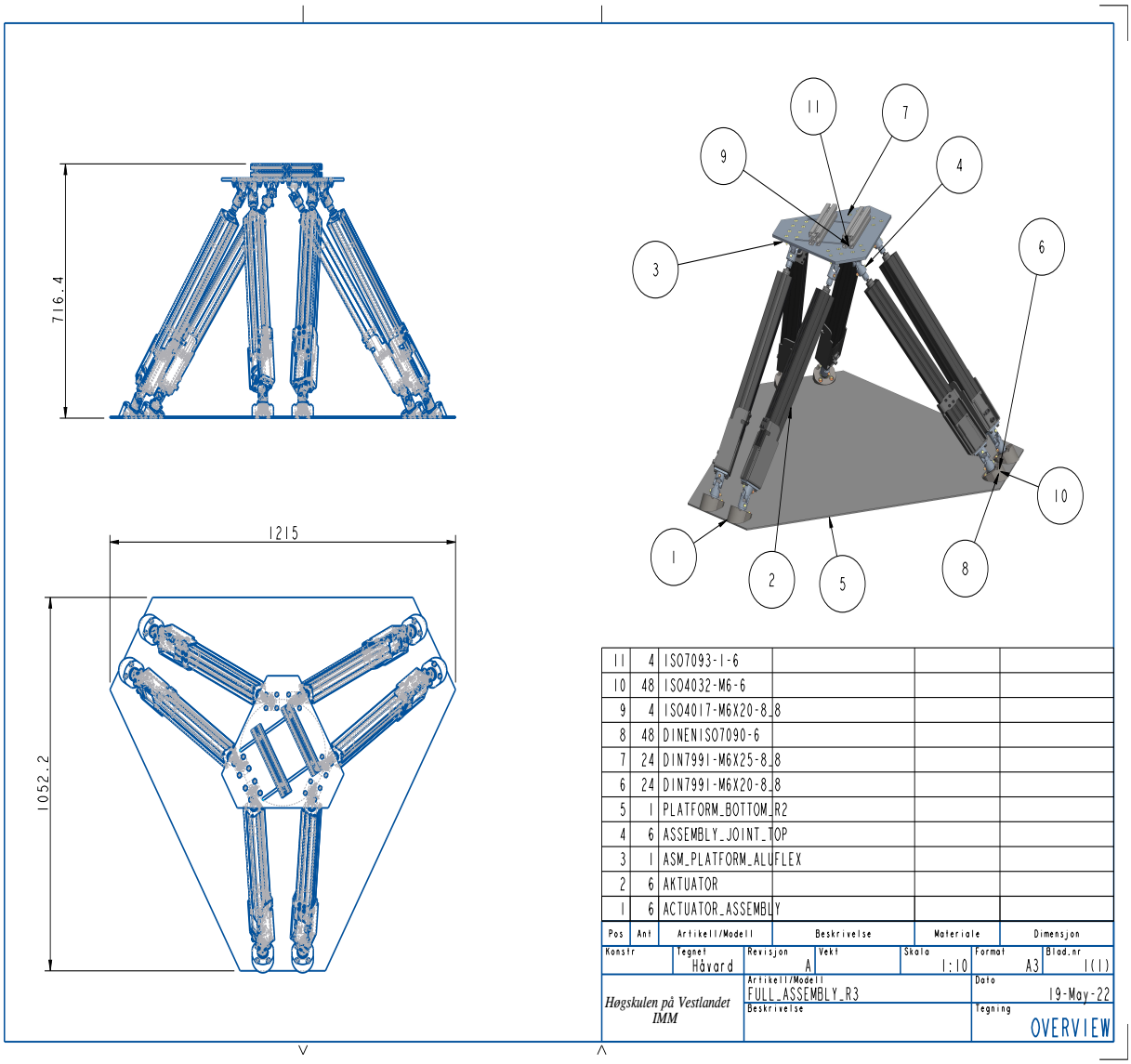


| Pos | Ant | Artikell/Modell | Beskrivelse | Materiale | Dimensjon |
|---|---|---|---|---|---|
| 11 | 4 | ISO7093-1-6 | | | |
| 10 | 48 | ISO4032-M6-6 | | | |
| 9 | 4 | ISO4017-M6X20-8.8 | | | |
| 8 | 48 | DINENISO7090-6 | | | |
| 7 | 24 | DIN7991-M6X25-8.8 | | | |
| 6 | 24 | DIN7991-M6X20-8.8 | | | |
| 5 | 1 | PLATFORM_BOTTOM_R2 | | | |
| 4 | 6 | ASSEMBLY_JOINT_TOP | | | |
| 3 | 1 | ASM_PLATFORM_ALUFLEX | | | |
| 2 | 6 | AKTUATOR | | | |
| 1 | 6 | ACTUATOR_ASSEMBLY | | | |

| | | | | | |
|---|---|---|---|---|---|
| Konstr | Tegnet Håvard | Revisjon A | Vekt | Skala 1:10 | Format A3 / Blad.nr 1(1) |
| *Høgskulen på Vestlandet IMM* | | Artikell/Modell FULL_ASSEMBLY_R3 | | | Dato 19-May-22 |
| | | Beskrivelse | | | Tegning OVERVIEW |

# Bearing housing assembly

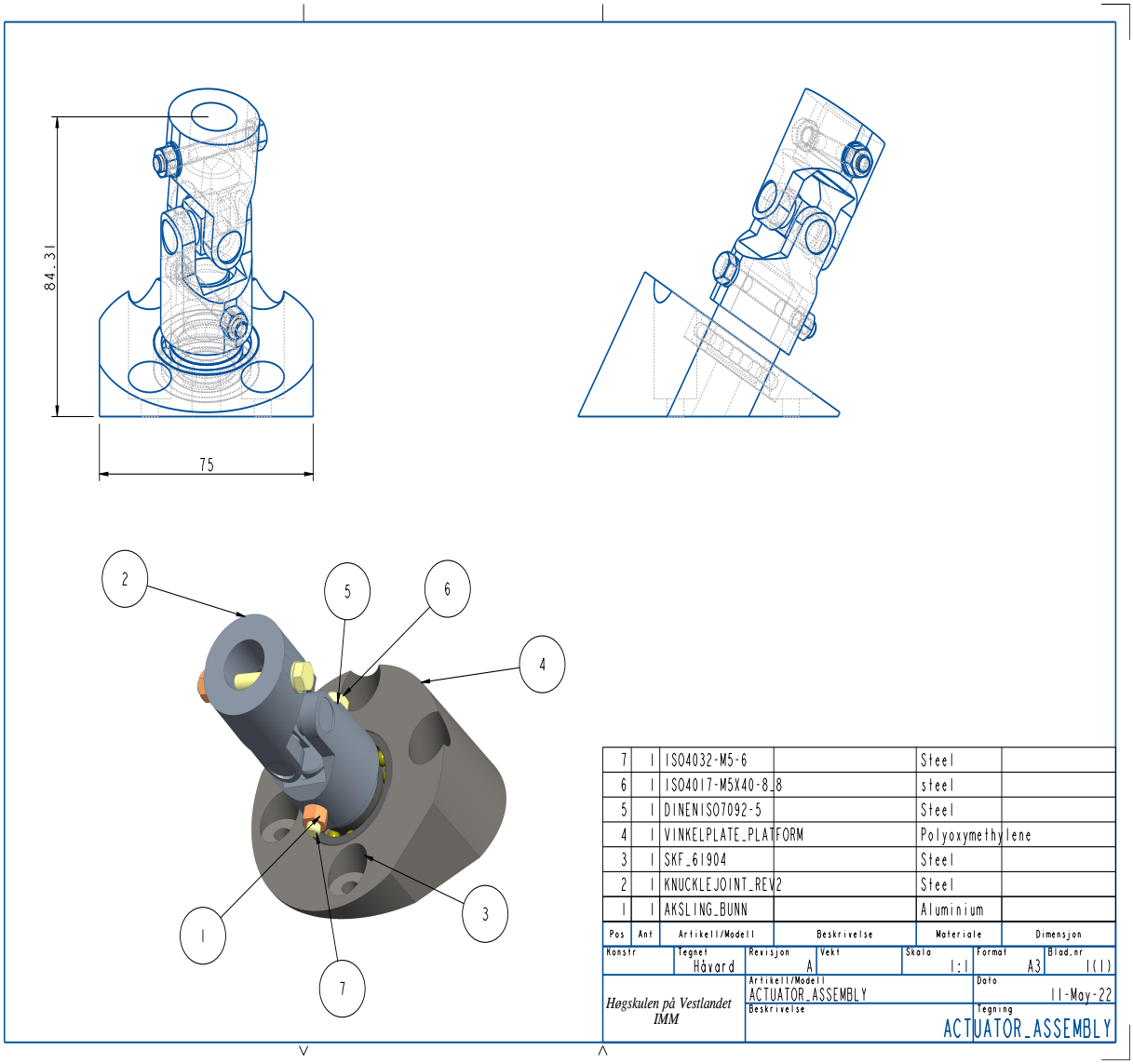


| Pos | Ant | Artikell/Modell | Beskrivelse | Materiale | Dimensjon |
|---|---|---|---|---|---|
| 7 | 1 | ISO4032-M5-6 | | Steel | |
| 6 | 1 | ISO4017-M5X40-8.8 | | steel | |
| 5 | 1 | DINENISO7092-5 | | Steel | |
| 4 | 1 | VINKELPLATE_PLATFORM | | Polyoxymethylene | |
| 3 | 1 | SKF_61904 | | Steel | |
| 2 | 1 | KNUCKLEJOINT_REV2 | | Steel | |
| 1 | 1 | AKSLING_BUNN | | Aluminium | |

| Konstr | Tegnet | Revisjon | Vekt | Skala | Format | Blad.nr |
|---|---|---|---|---|---|---|
| | Håvard | A | | 1:1 | A3 | 1(1) |

*Høgskulen på Vestlandet*
*IMM*

Artikell/Modell: ACTUATOR_ASSEMBLY
Beskrivelse:
Dato: 11-May-22
Tegning: ACTUATOR_ASSEMBLY

# Actuator assembly

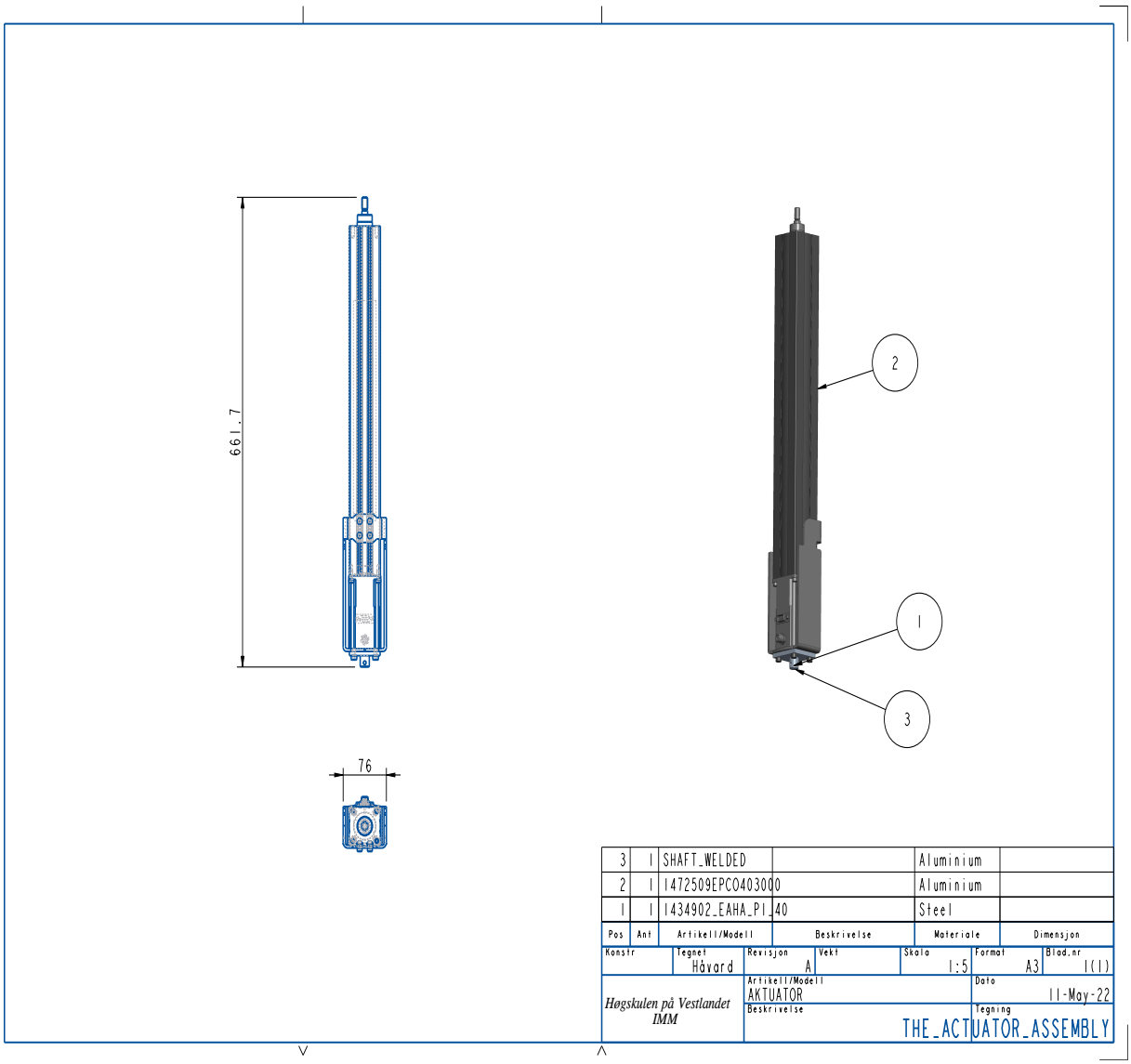

# Top-joint attachment assembly

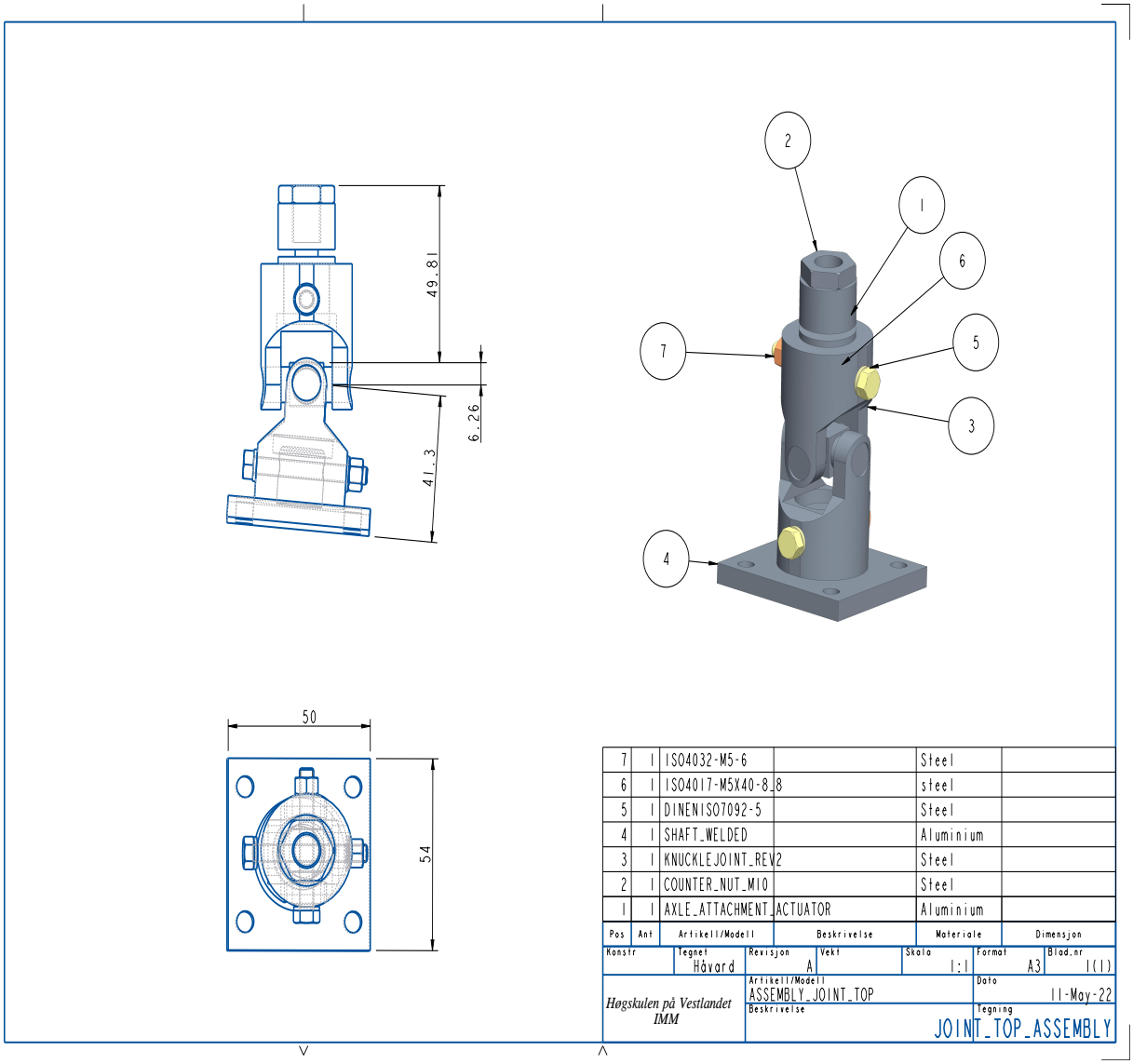


| Pos | Ant | Artikell/Modell | Beskrivelse | Materiale | Dimensjon |
|---|---|---|---|---|---|
| 7 | 1 | ISO4032-M5-6 | | Steel | |
| 6 | 1 | ISO4017-M5X40-8.8 | | steel | |
| 5 | 1 | DINENISO7092-5 | | Steel | |
| 4 | 1 | SHAFT_WELDED | | Aluminium | |
| 3 | 1 | KNUCKLEJOINT_REV2 | | Steel | |
| 2 | 1 | COUNTER_NUT_M10 | | Steel | |
| 1 | 1 | AXLE_ATTACHMENT_ACTUATOR | | Aluminium | |

| Konstr | Tegnet | Revisjon | Vekt | Skala | Format | Blad.nr |
|---|---|---|---|---|---|---|
| | Håvard | A | | 1:1 | A3 | 1(1) |

*Høgskulen på Vestlandet*
*IMM*

Artikell/Modell: ASSEMBLY_JOINT_TOP
Beskrivelse:
Dato: 11-May-22
Tegning: JOINT_TOP_ASSEMBLY

# Platform assembly

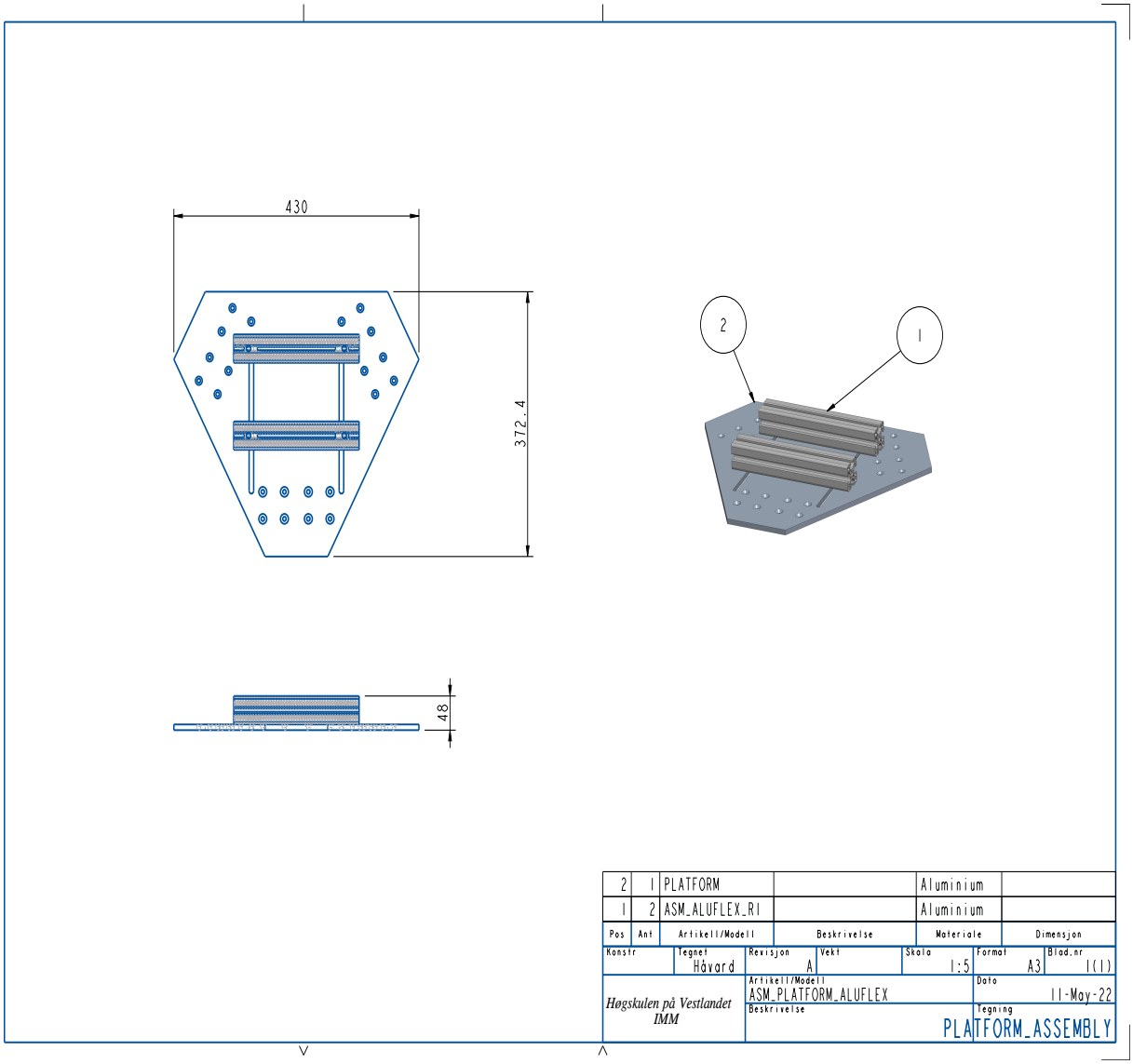


| Pos | Ant | Artikell/Modell | Beskrivelse | Materiale | Dimensjon |
|---|---|---|---|---|---|
| 2 | 1 | PLATFORM | | Aluminium | |
| 1 | 2 | ASM_ALUFLEX_R1 | | Aluminium | |

| | | | | | |
|---|---|---|---|---|---|
| Konstr | Tegnet: Håvard | Revisjon: A | Vekt | Skala: 1:5 | Format: A3 / Blad.nr: 1(1) |
| *Høgskulen på Vestlandet IMM* | | Artikell/Modell: ASM_PLATFORM_ALUFLEX | | | Dato: 11-May-22 |
| | | Beskrivelse | | | Tegning: PLATFORM_ASSEMBLY |

# Platform

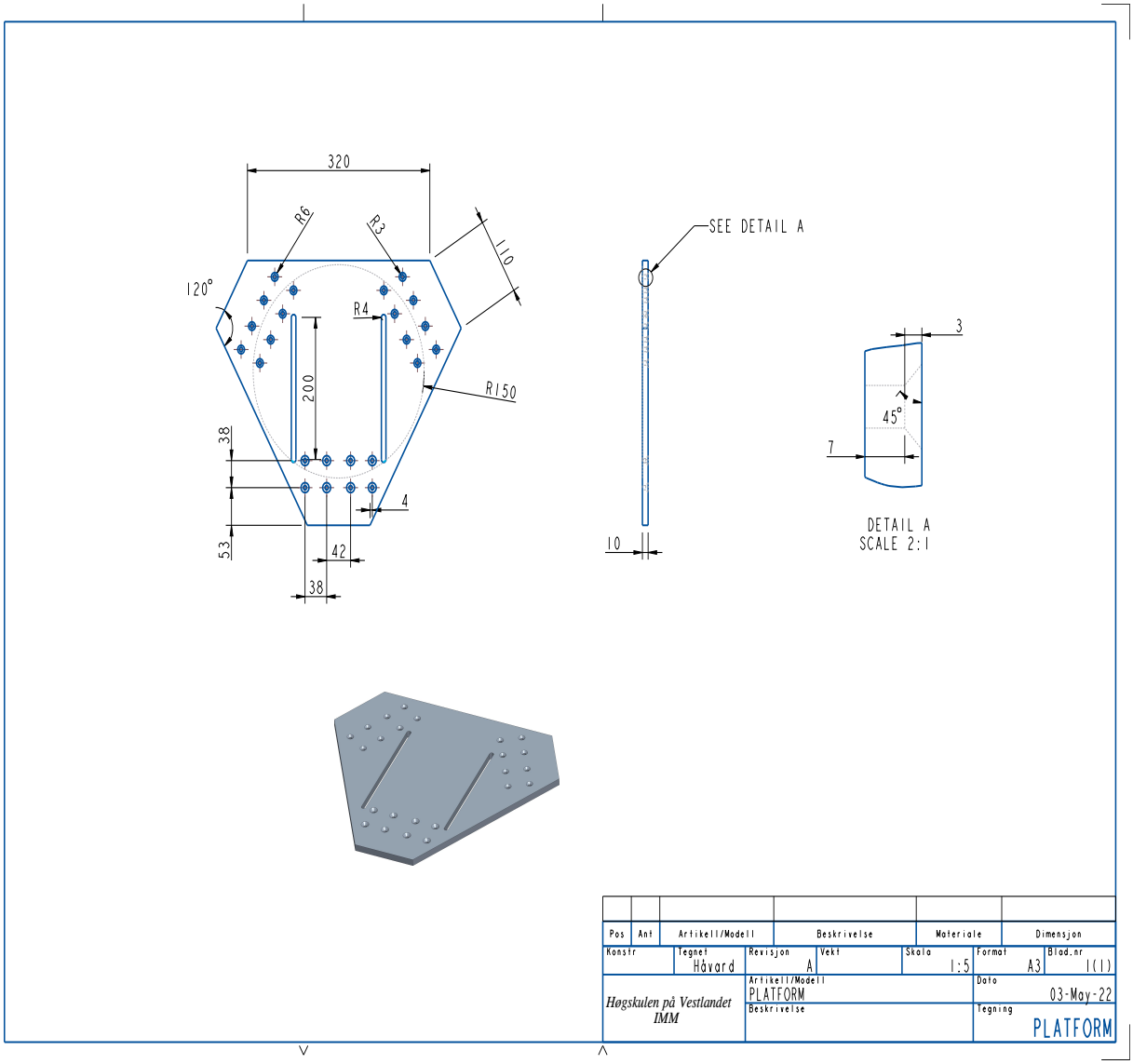
320
R6
R3
110
120°
R4
200
R150
38
4
53
42
38
SEE DETAIL A
10
3
45°
7
DETAIL A
SCALE 2:1
Pos
Ant
Artikell/Modell
Beskrivelse
Materiale
Dimensjon
Konstr
Tegnet
Håvard
Revisjon
A
Vekt
Skala
1:5
Format
A3
Blad.nr
1(1)
Høgskulen på Vestlandet
IMM
Artikell/Modell
PLATFORM
Beskrivelse
Dato
03-May-22
Tegning
PLATFORM

# Bearing housing

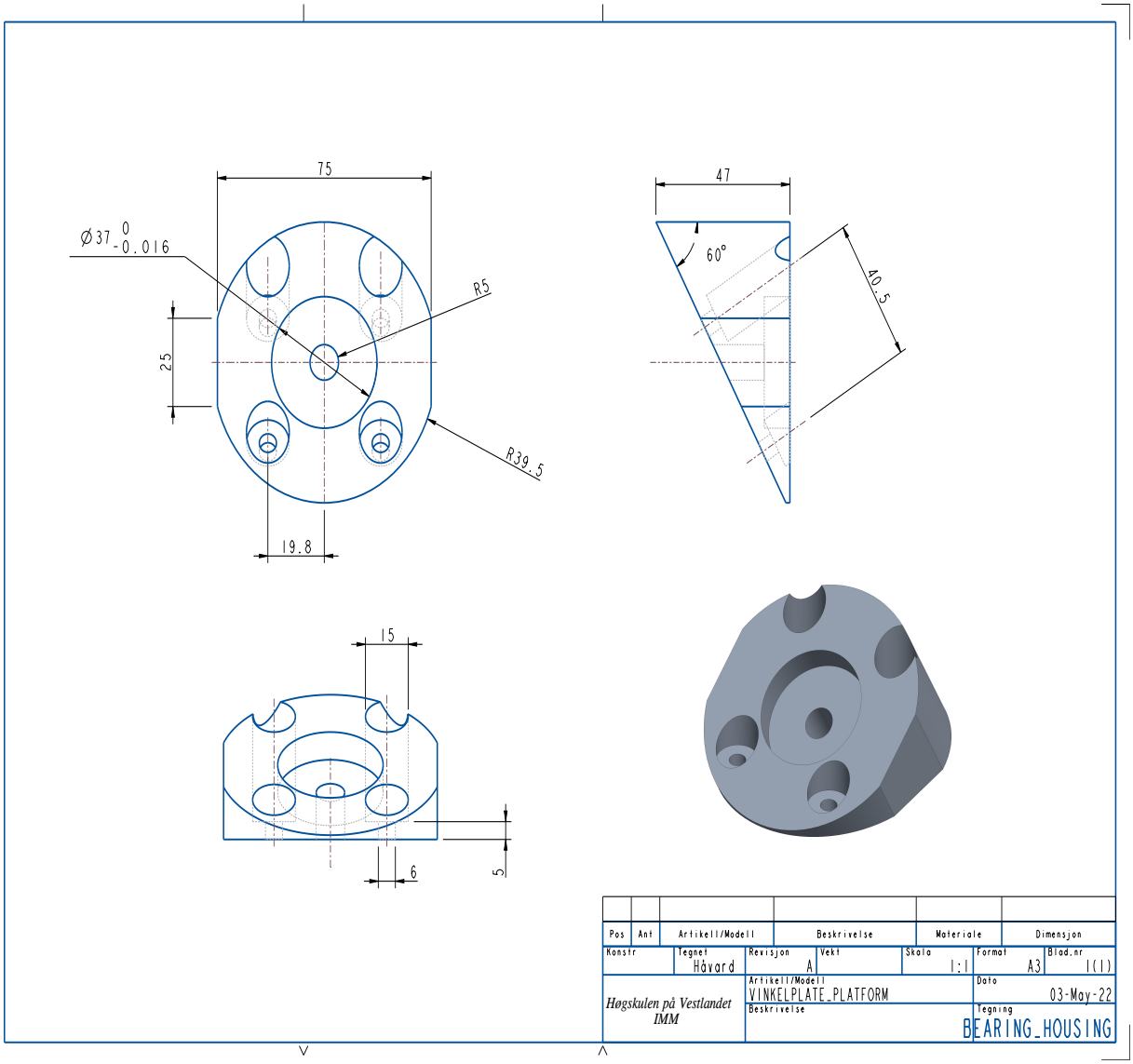

# Bearing shaft

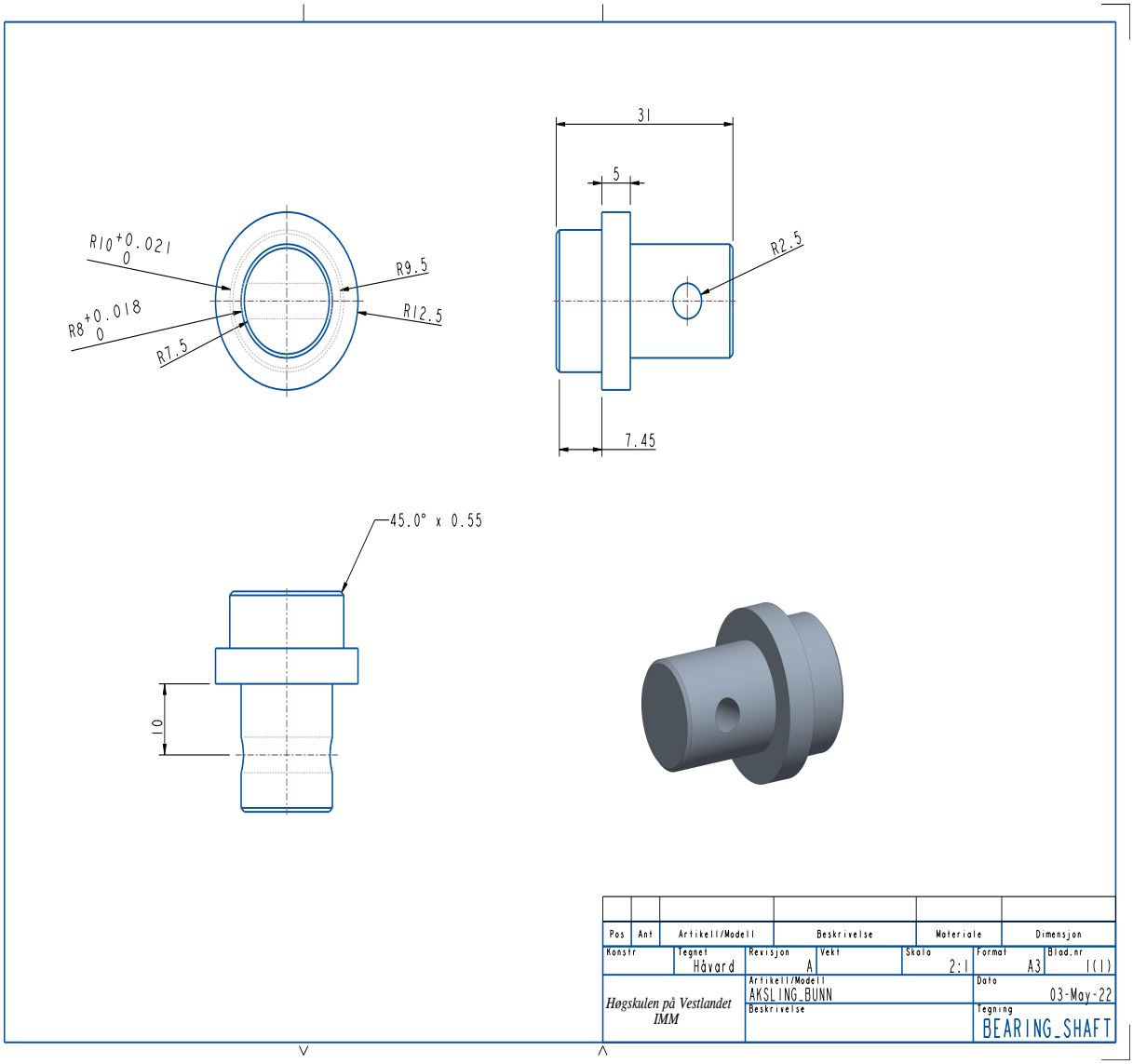

# Shaft with notch

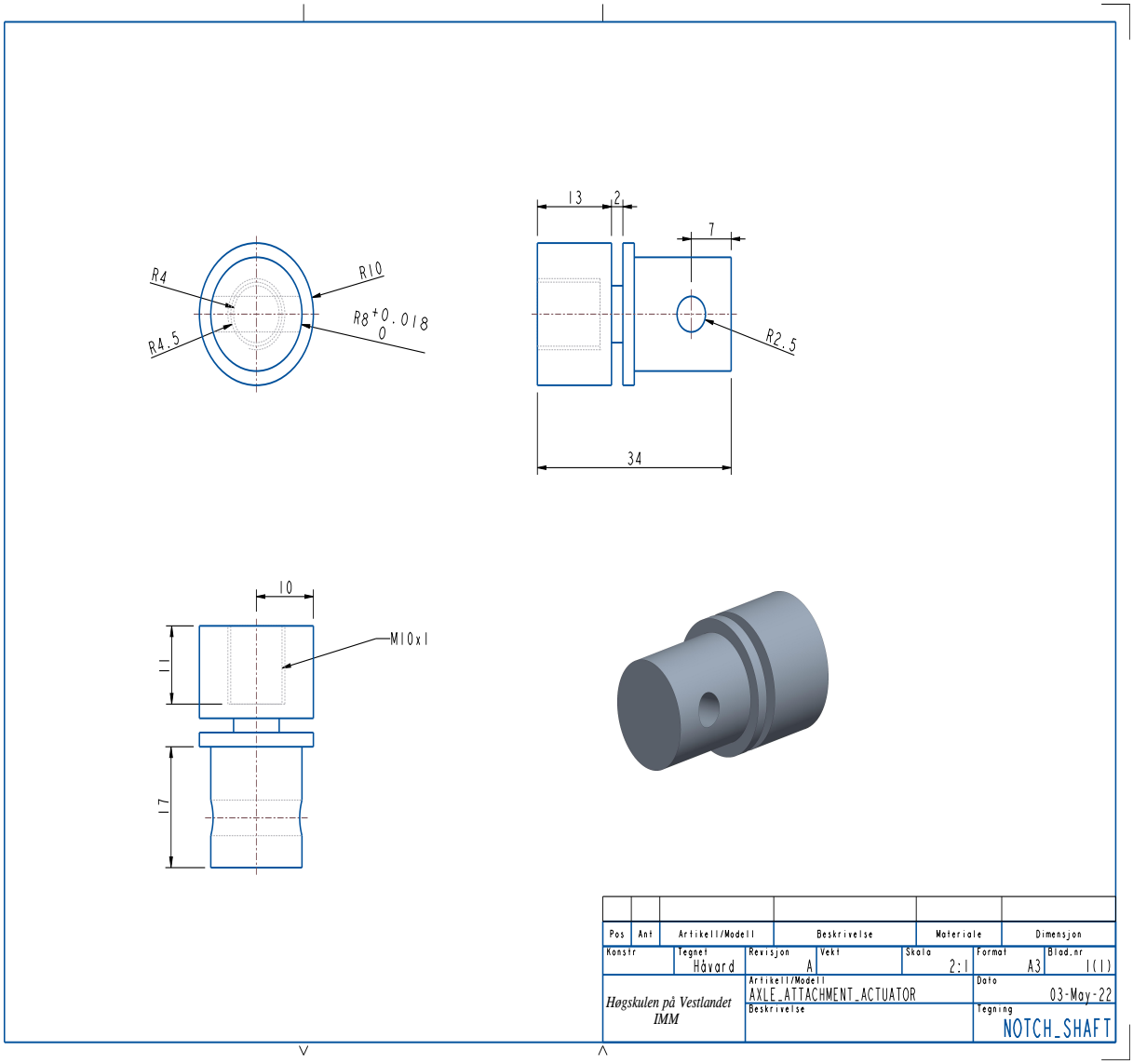

# Milled shaft

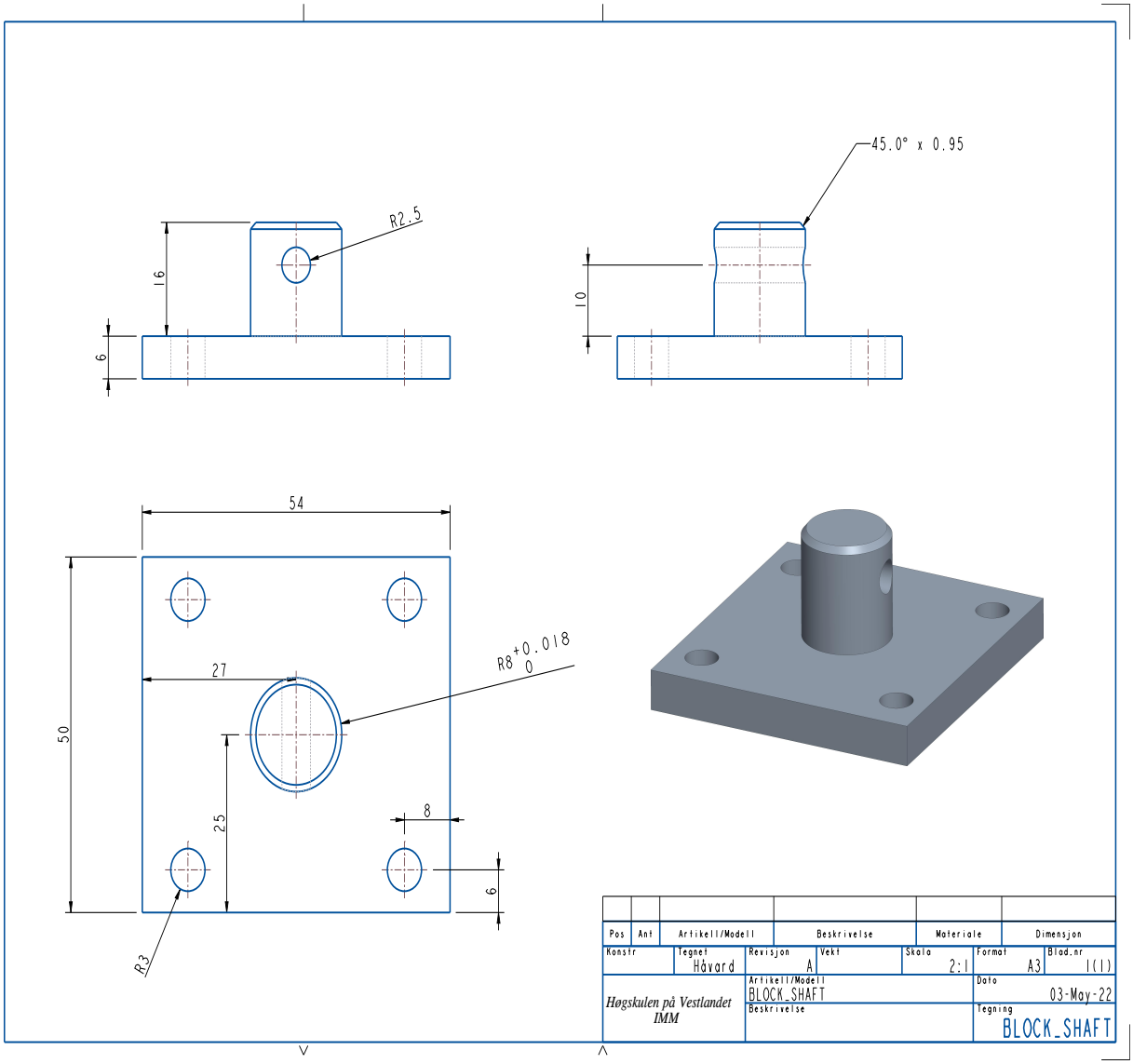

# Corner bracket

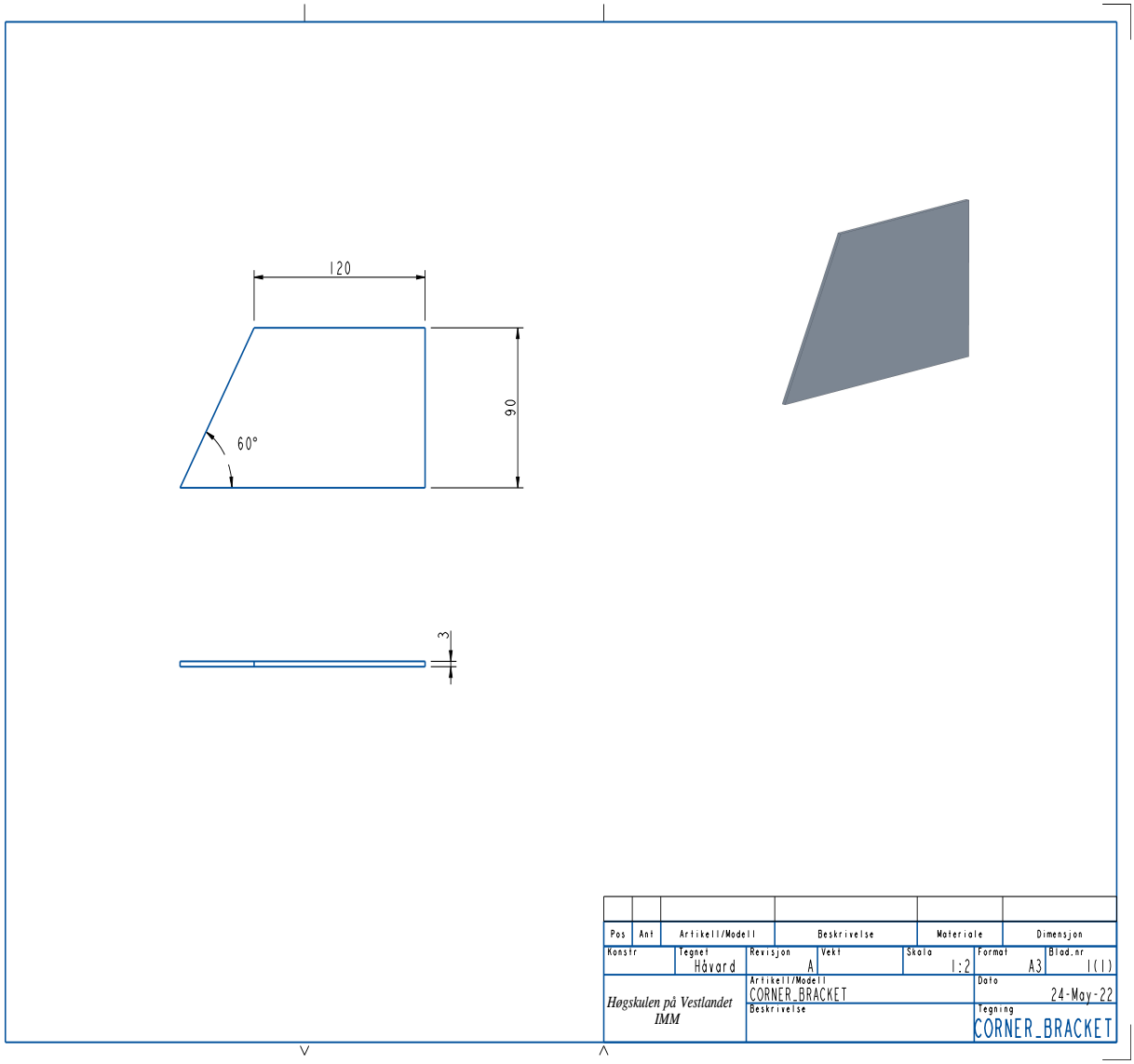

# Appendix B: MATLAB script

## Appendix B1. Stewart platform visualization

```
close all;
clc;
X=0;
Y=0;
Z=1;
yaw=90*pi/180;
roll=0*pi/180;
pitch=0*pi/180;
%syms X Y Z yaw roll pitch
Px1=X+(3140116564492417*cos(roll)*cos(yaw))
   /72057594037927936+(4486462071114449*cos(pitch)*sin(yaw))
   /9007199254740992+(4486462071114449*cos(yaw)*sin(pitch)*sin(roll
   ))/9007199254740992;
Py1=Y-(4486462071114449*cos(pitch)*cos(yaw))
   /9007199254740992+(3140116564492417*cos(roll)*sin(yaw))
   /72057594037927936+(4486462071114449*sin(pitch)*sin(roll)*sin(
   yaw))/9007199254740992;
Pz1=Z+(3140116564492417*sin(roll))
   /72057594037927936-(4486462071114449*cos(roll)*sin(pitch))
   /9007199254740992;
Px2=X+(8163294823962471*cos(roll)*cos(yaw))
   /18014398509481984-(7613213784381523*cos(pitch)*sin(yaw))
   /36028797018963968-(7613213784381523*cos(yaw)*sin(pitch)*sin(
   roll))/36028797018963968;
Py2=Y+(7613213784381523*cos(pitch)*cos(yaw))
   /36028797018963968+(8163294823962471*cos(roll)*sin(yaw))
   /18014398509481984-(7613213784381523*sin(pitch)*sin(roll)*sin(
   yaw))/36028797018963968;
Pz2=Z+(8163294823962471*sin(roll))
   /18014398509481984+(7613213784381523*cos(roll)*sin(pitch))
   /36028797018963968;
Px3=X+(7378265682839367*cos(roll)*cos(yaw))
   /18014398509481984-(645789656254767*cos(pitch)*sin(yaw))
   /2251799813685248-(645789656254767*cos(yaw)*sin(pitch)*sin(roll)
   )/2251799813685248;
Py3=Y+(645789656254767*cos(pitch)*cos(yaw))
   /2251799813685248+(7378265682839367*cos(roll)*sin(yaw))
   /18014398509481984-(645789656254767*sin(pitch)*sin(roll)*sin(yaw
```

```
   ))/2251799813685248;
Pz3=Z+(7378265682839367*sin(roll))
   /18014398509481984+(645789656254767*cos(roll)*sin(pitch))
   /2251799813685248;
Px4=X-(7378265682839367*cos(roll)*cos(yaw))
   /18014398509481984-(645789656254767*cos(pitch)*sin(yaw))
   /2251799813685248-(645789656254767*cos(yaw)*sin(pitch)*sin(roll)
   )/2251799813685248;
Py4=Y+(645789656254767*cos(pitch)*cos(yaw))
   /2251799813685248-(7378265682839367*cos(roll)*sin(yaw))
   /18014398509481984-(645789656254767*sin(pitch)*sin(roll)*sin(yaw
   ))/2251799813685248;
Pz4=Z-(7378265682839367*sin(roll))
   /18014398509481984+(645789656254767*cos(roll)*sin(pitch))
   /2251799813685248;
Px5=X-(8163294823962471*cos(roll)*cos(yaw))
   /18014398509481984-(7613213784381523*cos(pitch)*sin(yaw))
   /36028797018963968-(7613213784381523*cos(yaw)*sin(pitch)*sin(
   roll))/36028797018963968;
Py5=Y+(7613213784381523*cos(pitch)*cos(yaw))
   /36028797018963968-(8163294823962471*cos(roll)*sin(yaw))
   /18014398509481984-(7613213784381523*sin(pitch)*sin(roll)*sin(
   yaw))/36028797018963968;
Pz5=Z-(8163294823962471*sin(roll))
   /18014398509481984+(7613213784381523*cos(roll)*sin(pitch))
   /36028797018963968;
Px6=X-(3140116564492417*cos(roll)*cos(yaw))
   /72057594037927936+(4486462071114449*cos(pitch)*sin(yaw))
   /9007199254740992+(4486462071114449*cos(yaw)*sin(pitch)*sin(roll
   ))/9007199254740992;
Py6=Y-(4486462071114449*cos(pitch)*cos(yaw))
   /9007199254740992-(3140116564492417*cos(roll)*sin(yaw))
   /72057594037927936+(4486462071114449*sin(pitch)*sin(roll)*sin(
   yaw))/9007199254740992;
Pz6=Z-(3140116564492417*sin(roll))
   /72057594037927936-(4486462071114449*cos(roll)*sin(pitch))
   /9007199254740992;
Bz(1:6)=0;
%Calculated Length of each Leg
L1=sqrt((Px1-Bx(6))^2+(Py1-By(6))^2+(Pz1-Bz(6))^2);
L2=sqrt((Px2-Bx(1))^2+(Py2-By(1))^2+(Pz2-Bz(1))^2);
L3=sqrt((Px3-Bx(2))^2+(Py3-By(2))^2+(Pz3-Bz(2))^2);
```

```
L4=sqrt((Px4-Bx(3))^2+(Py4-By(3))^2+(Pz4-Bz(3))^2);
L5=sqrt((Px5-Bx(4))^2+(Py5-By(4))^2+(Pz5-Bz(4))^2);
L6=sqrt((Px6-Bx(5))^2+(Py6-By(5))^2+(Pz6-Bz(5))^2);
%To find the jacobian the syms must be used..
% j=simple(jacobian([L1 L2 L3 L4 L5 L6],[X Y Z yaw roll pitch]))
axis([-1 1 -1 1 0 2])
hold on
%plotting lines between joints of the base
line([Bx(1) Bx(2)],[By(1) By(2)],[Bz(1) Bz(2)]);
line([Bx(2) Bx(3)],[By(2) By(3)],[Bz(2) Bz(3)]);
line([Bx(3) Bx(4)],[By(3) By(4)],[Bz(3) Bz(4)]);
line([Bx(4) Bx(5)],[By(4) By(5)],[Bz(4) Bz(5)]);
line([Bx(5) Bx(6)],[By(5) By(6)],[Bz(5) Bz(6)]);
line([Bx(6) Bx(1)],[By(6) By(1)],[Bz(6) Bz(1)]);
%plotting lines between joints of the platform
line([Px1 Px2],[Py1 Py2],[Pz1 Pz2]);
line([Px2 Px3],[Py2 Py3],[Pz2 Pz3]);
line([Px3 Px4],[Py3 Py4],[Pz3 Pz4]);
line([Px4 Px5],[Py4 Py5],[Pz4 Pz5]);
line([Px5 Px6],[Py5 Py6],[Pz5 Pz6]);
line([Px6 Px1],[Py6 Py1],[Pz6 Pz1]);
plotting Joints of platform
plot3(Px1,Py1,Pz1,'ro');
plot3(Px2,Py2,Pz2,'ro');
plot3(Px3,Py3,Pz3,'ro');
plot3(Px4,Py4,Pz4,'ro');
plot3(Px5,Py5,Pz5,'ro');
plot3(Px6,Py6,Pz6,'ro');
plotting Joints of base
plot3(Bx(1),By(1),Bz(1),'ro');
plot3(Bx(2),By(2),Bz(2),'ro');
plot3(Bx(3),By(3),Bz(3),'ro');
plot3(Bx(4),By(4),Bz(4),'ro');
plot3(Bx(5),By(5),Bz(5),'ro');
plot3(Bx(6),By(6),Bz(6),'ro');
%plotting LEGS
line([Px1 Bx(6)],[Py1 By(6)],[Pz1 Bz(6)],'color','g');
line([Px2 Bx(1)],[Py2 By(1)],[Pz2 Bz(1)],'color','g');
line([Px3 Bx(2)],[Py3 By(2)],[Pz3 Bz(2)],'color','g');
line([Px4 Bx(3)],[Py4 By(3)],[Pz4 Bz(3)],'color','g');
line([Px5 Bx(4)],[Py5 By(4)],[Pz5 Bz(4)],'color','g');
line([Px6 Bx(5)],[Py6 By(5)],[Pz6 Bz(5)],'color','g');
```

## Appendix B2. Wave data analysis

```
clear all
clc
close all
%% Description
%   t, t2 are time steps for the range, velocity/speed
%
%   This script turns range data from MarinLab into velocity,
%   ... and speed by differnetiating and dividing by the time step
%
%
%% Reading file
dirName="filter1.tsv"; % replace .tsv file name with any MarinLab
   file
data_s4 = readfromline(dirName, 15, 18); % if error at this line,
   check heading of .tsv, or name of file

%% Position data
t = data_s4(:,2);     % Time (used for range plots)

x = data_s4(:,3);     % X-position (mm)
y = data_s4(:,4);     % Y-position (mm)
z = data_s4(:,5);     % Z-position (mm)

yaw = abs(data_s4(:,6));
pitch = data_s4(:,7);
roll = data_s4(:,8);
```